

AD-A097 362

CALIFORNIA INST OF TECH PASADENA ANTENNA LAB F/G 18/6
THE DEVELOPMENT AND APPLICATION OF NOVEL METHODS FOR THE SOLUTI--ETC(U)
FEB 81 C H PAPAS AFOSR-77-3451

UNCLASSIFIED

AFOSR-TR-81-0336

NL

[CP]
ADA
097 362

01

END
DATE
FILMED
5-81
DTIC

AFO/R-TR- 81 - 0336

LEVEL *II*

(11)

CALIFORNIA INSTITUTE OF TECHNOLOGY

ANTENNA LABORATORY

*THE DEVELOPMENT AND APPLICATION OF NOVEL
METHODS FOR THE SOLUTION OF EMP
SHIELDING PROBLEMS*

FINAL SCIENTIFIC REPORT
Grant AFOSR-77-3451

by

C. H. Papas

AD A097362

DTIC FILE COPY

DTIC
ECTE
APR 6 1981
C

February 1981

81 4

6 005

Approved for public release; -
distribution unlimited.

UNCLASSIFIED

SECURITY CLASSIFICATION OF THIS PAGE (When Data Entered)

REPORT DOCUMENTATION PAGE		READ INSTRUCTIONS BEFORE COMPLETING FORM	
1. REPORT NUMBER (18) AFOSR-81-0336	2. GOVT ACCESSION NO. AD-A097362	3. REPORT'S CATALOG NUMBER	
4. TITLE (and Subtitle) (6) THE DEVELOPMENT AND APPLICATION OF NOVEL METHODS FOR THE SOLUTION OF EMP SHIELDING PROBLEMS		5. TYPE OF REPORT & PERIOD COVERED (11) Final rept.	
7. AUTHOR(s) (10) Charles H. Papas		8. CONTRACT OR GRANT NUMBER(s) (15) AFOSR-77-3451	
9. PERFORMING ORGANIZATION NAME AND ADDRESS Department of Electrical Engineering California Institute of Technology Pasadena, CA 91125		10. PROGRAM ELEMENT, PROJECT, TASK AREA & WORK UNIT NUMBERS 61102F (16) 2301A3	
11. CONTROLLING OFFICE NAME AND ADDRESS AFOSR/NP Bolling AFB Wash DC 20332		12. REPORT DATE (11) Feb 81	
14. MONITORING AGENCY NAME & ADDRESS (if different from Controlling Office) (17) A3 (12) 137		13. NUMBER OF PAGES 35	
		15. SECURITY CLASS. (of this report) unclassified	
		15a. DECLASSIFICATION/DOWNGRADING SCHEDULE	
16. DISTRIBUTION STATEMENT (of this Report) Approved for public release; distribution unlimited.			
17. DISTRIBUTION STATEMENT (of the abstract entered in Block 20, if different from Report)			
18. SUPPLEMENTARY NOTES			
19. KEY WORDS (Continue on reverse side if necessary and identify by block number)			
20. ABSTRACT (Continue on reverse side if necessary and identify by block number) The purpose of this report is to summarize the electromagnetic research that was performed through the support of AFOSR. The problems worked on pertain to EMP shielding theory and deal with a. the transmission of electromagnetic waves through small apertures, b. the propagation of electromagnetic waves through chiral media, c. the steady state and transient electromagnetic coupling through slabs, and d. the pondermotive forces and torques produced by electromagnetic waves.			

DD FORM 1 JAN 73 1473

EDITION OF 1 NOV 65 IS OBSOLETE

UNCLASSIFIED

030750

SECURITY CLASSIFICATION OF THIS PAGE (When Data Entered)

11

Final Scientific Report

submitted by

C. H. Papas

California Institute of Technology

Pasadena, California

SECRET

A Final Report to U. S. Air Force Office of Scientific Research
Summarizing Research Performed Under
Grant AFOSR-77-3451

February 1981

AIR FORCE OFFICE OF SCIENTIFIC RESEARCH (AFSC)
NOTICE OF TRANSMITTAL TO DOD
THIS DOCUMENT HAS BEEN REVIEWED AND IS
APPROVED FOR RELEASE IAW AFR 190-12 (7b).
DISTRIBUTION UNLIMITED.
A. D. Black
Technical Information Officer

Introduction

It is the purpose of this report to summarize the electromagnetic research we have performed through the kind support of the AFOSR. The problems we have worked on pertain to EMP shielding theory and deal with

- a) the transmission of electromagnetic waves through small apertures,
- b) the propagation of electromagnetic waves through chiral media,
- c) the steady state and transient electromagnetic coupling through slabs, and
- d) the pondermotive forces and torques produced by electromagnetic waves.

In what follows we describe the problems we investigated and the results we obtained. The details of our work were circulated among the cognizant officers of the Weapons Laboratory, Kirtland Air Force Base, New Mexico and then published in the open literature. A full discussion of our calculations can be found in our published papers, photocopies of which are attached to this report.

Accession For	
NTIS GRA&I	<input checked="checked" type="checkbox"/>
DTIC TAB	<input type="checkbox"/>
Unannounced	<input type="checkbox"/>
Justification	
By	
Distribution/	
Availability Codes	
Avail and/or	
Dist	Special
A	

Small Apertures

The question of how much of the electromagnetic energy that exists on one side of a wall can leak to the other side through a small opening in the wall is, by virtue of its practical importance, a canonical problem in EMP shielding theory.

For an opening that is circular, the answer is known from the celebrated works of Rayleigh, Bethe, Bouwkamp, Meixner, and Andrejewski. However, for a non-circular opening it appears impossible to solve the problem exactly, unless the opening has a shape that is simple enough to permit a separation of the variables and a scalarization of the field. This means that for most openings of practical interest an exact solution can not be found and one must handle the problem by a method of approximation.

One can formulate the problem so that upper and lower bounds on the true (exact) solution and not the true solution itself need be found. Such a formulation can be based on Levine and Schwinger's discovery that when the aperture (of any shape) is electrically small there exists a variational principle for the upper bound and a variational principle for the lower bound. This variational approach can yield accurate results but in general does not lend itself to easy calculation.

In our work we discovered a simpler method of sandwiching the true solution between upper and lower bounds, namely, the method of symmetrization which has yielded important results in geometry. We developed the method in the direction of electromagnetics and applied it to our aperture problem. One of our principal results is given by the simple formula

$$\tau \leq \frac{68(P/\lambda)^6}{27\pi^3(A/\lambda^2)}$$

for the transmission through an aperture of area A and perimeter P . Here τ is the transmission coefficient and λ is the wavelength.

From this formula we see that when an aperture of given area is symmetrized the aperture's perimeter decreases and the maximum possible transmission decreases as the shape of the aperture approaches that of a circle. For example, the maximum possible transmission decreases as the shape of the aperture is changed from that of an equilateral triangle to that of a square and finally to that of a circle.

For a full discussion of the method of symmetrization and its application to EMP shielding the reader is invited to read: D. L. Jaggard and C. H. Papas: "On the Application of Symmetrization to the Transmission of Electromagnetic Waves Through Small Convex Apertures of Arbitrary Shape", Applied Physics 15, 21-25 (1978).

Chiral Media

Chirality is a purely geometric notion which refers to the lack of symmetry of an object. By definition, an object is chiral if it cannot be brought into congruence with its mirror image by translation and rotation. An object that is not chiral is said to be achiral. Some chiral objects occur naturally in two versions one being the chiral object and the other being its mirror image. Such objects are said to be enantiomorphs of each other.

A chiral object has the property of handedness; it must be either left-handed or right-handed. The handedness of helices was demonstrated by W. H. Pickering. His experimental results showed that a collection of randomly oriented left-handed helices would rotate the plane of polarization of a linearly polarized microwave one way whereas a collection of right-handed helices would rotate the plane of polarization the opposite way.

As a generalization of Pickering's results, our research led us to the following conjecture: Any medium composed of randomly oriented equivalent chiral objects will rotate the plane of polarization one way, say, to the left, while a medium composed of the enantiomorphs of these objects will rotate the plane of polarization the opposite way, i.e. to the right. By examining the

wire helix and the wire braid as chiral objects, we obtained results which support this conjecture. Moreover, we showed that the pondermotive forces on the helix and the braid tend to reduce their chirality.

The practical applicability of chirality to the measurement of EMP was studied and several experiments based on the concept of chirality were designed.

For further details please read:

D. L. Jaggard, A. R. Mickelson, and C. H. Papas, "On Electromagnetic Waves in Chiral Media", Applied Physics 18, 211-216 (1979).

Slab Coupling

We studied the problem of transmission of steady-state and transient electromagnetic waves through a slab. An analytical solution was obtained for the case of a linear homogeneous, isotropic, highly conducting, infinite slab excited by collinear electric or magnetic dipoles.

We found that the transmitted components of the field are given as the product (steady-state case) or the convolution (transient case) of the corresponding incident field components and a two-term factor. In the frequency domain the first term of this factor is exactly the transmission coefficient of a plane wave normally incident on the slab. The second term of this factor brings into play the finite distance between the transmitting and receiving antennas and becomes significant only when this distance is of the order of, or smaller than, the free-space wavelength (steady-state case) or the spatial wavelength of the incident pulse (transient case). Accordingly, we showed that it is possible to obtain plane wave excitation results even when the sources and the receivers are located at finite distances.

We derived the conditions under which measurements made with source and receiver at finite distances are equivalent to the same measurements made with plane wave excitation.

This work has been applied to the laboratory testing of EMP slab coupling.

For further details we refer the reader to:

G. Franceschetti and C. H. Papas, "Steady State and Transient Electromagnetic Coupling Through Slabs", IEEE Trans. vol.AP-27, No. 5, September 1979.

Pondermotive Forces

It is well known that an electromagnetic wave exerts forces and (possibly) torques on charges and currents and that the mathematical description of these mechanical actions is given by the Lorentz force equation, which connects electromagnetic and mechanical phenomena. If an electromagnetic wave interacts with, say, a metal body, charges and currents are induced, and hence the body becomes subject to local forces and torques. When a spatial summation is made, the total time-dependent (body) force and (body) torque acting on the object are obtained. It is usually believed that these forces and torques are "small" and hence negligible from the viewpoint of engineering application. However, this is not always so. As a matter of fact, a strong interest in this area is now emerging.

Electromagnetic pulses (EMP) produced by nuclear explosion in the upper atmosphere is a case of recent interest. Also satellite applications have attracted considerable attention, where the (relatively) small mass of the object and the cumulative nature of the mechanical actions (translation or rotation) can produce long-range macroscopic effects. Mechanical effects can be used, for example, to steer the satellite by radiating suitably polarized electromagnetic fields from the satellite. And even key operations, as deploying antennas, can be performed, in principle, by injecting transient currents into the structures. There are cases in which the movement of a metal object in an electromagnetic field can produce additional mechanical stresses. For instance, the propellers of a helicopter, which may be roughly modeled as rotating dipoles, can be further stressed when exposed to an incident electromagnetic field. Clearly related is the problem of the electromagnetic gun.

Accordingly, we examined a number of very simple cases of interaction between metal objects and electromagnetic fields, and computed the resulting mechanical

forces and torques. As the metal object, we considered the simplest one -- the tuned electric dipole -- in several configurations: stationary, translational, rotational, receiving, transmitting, where the electric dipole was isolated or coupled with a magnetic dipole as a turnstile antenna or a chiral antenna. We computed the body force and torque acting on the dipole and its time average, for the case of an incident, or a transmitted, harmonic electromagnetic field. As a general result, the forces are always proportional to the Poynting vector (divided by the velocity of light) times an "equivalent area", which is four times larger than the usual effective area -- $3\lambda^2/4\pi$ -- of the (tuned) dipole. This clearly implies that the mechanical action depends on the power scattered by the dipole. Similarly, the torque is proportional to the Poynting vector (divided by the angular frequency of the wave) times the same equivalent area. The existence of the torque, however, is not dependent only on the symmetry properties of the scattering object or on the polarization of the incident wave. We examined cases in which the incident field -- circularly polarized -- carries an angular momentum and yet exerts no torque on the dipole. Conversely, we examined cases in which the dipole -- a simple short wire -- radiates as a scattered field a linearly polarized wave (in the far-field) and has torques exerted on it. The full analysis of a rigorous boundary value problem -- a metal sphere in an incident field -- showed that the transient force has not always the same sense as the incident radiation; in other words, the sphere is alternately pushed and pulled in the direction of the incident Poynting vector. The large variety of effects we discovered in this "case" analysis seems to indicate that this is an underdeveloped field of very interesting research, and a number of general theorems could probably be discovered, thus bringing to a better understanding of a wrongly neglected field.

For a full discussion of our work on this subject please see:

G. Franceschetti and C. H. Papas, "Mechanical Forces and Torques Associated With Electromagnetic Waves", Applied Physics 23, 153-161 (1980).

Final Remarks and Acknowledgment

Under this grant we solved a number of electromagnetic problems that had been raised to positions of importance by their relevance to EMP shielding.

We handled the problems analytically and not by computer so that greater insight into the attendant physical phenomena would be gained.

The solutions we obtained were deduced from Maxwell's equations by rather novel methods and concepts. For each problem the analysis was carried to completion, i.e. to a point where a formula or global statement of design importance was obtained. Thus we feel that we have contributed not only to the overall problem of EMP shielding but also to the advancement of applied electromagnetic theory.

The members of our research group at Caltech who worked on these problems (G. Franceschetti, D. L. Jaggard, A. R. Mickelson, and C. H. Papas) sincerely appreciate the assistance and cooperation of Dr. J. P. Castillo of the Air Force Weapons Laboratory and Dr. Kelvin Lee of the Dikewood Corporation.

Also many thanks are due Dr. Michael G. Harrison of the Air Force Weapons Laboratory for his kind and efficient service as project officer.

On the Application of Symmetrization to the Transmission of Electromagnetic Waves Through Small Convex Apertures of Arbitrary Shape

D. L. Jaggard and C. H. Papas

Division of Engineering and Applied Science, California Institute of Technology, Pasadena, CA 91125, USA

Received 9 August 1977 Accepted 20 September 1977

Abstract. The transmission of an electromagnetic wave through a small aperture in a perfectly conducting screen is examined from the viewpoint of symmetrization.

PACS: 02, 41

The question of how much of the electromagnetic energy that exists on one side of a wall can leak to the other side through a small opening in the wall has become, by virtue of its practical importance, a canonical problem in the theory of EMP (electromagnetic pulse) interactions [1].

As is well known, the earliest calculation of the transmission of an electromagnetic wave through a small circular aperture in a plane screen of perfect conductivity and zero thickness was performed by Lord Rayleigh. Using potential theory, he calculated the transmitted field of a plane harmonic wave normally incident on an electrically small circular aperture [2]. Years later Bethe derived expressions for the polarizabilities and effective dipole moments of small circular apertures. His results give the transmitted far field for any angle of incidence but not the transmitted near field [3]. Most recently Bouwkamp [4], Meixner and Andrejewski [5], and Andrejewski [6] found an exact solution for both the near and far transmitted fields of a plane wave normally incident on a circular aperture.

Aperture problems can, at least in principle, be solved numerically, but they cannot be solved analytically unless the shape of the aperture happens to be simple enough to permit a separation of the variables and a scalarization of the electromagnetic field. However, from this it should not be inferred that if the aperture problem cannot be solved analytically, a numerical method is the only way to obtain a solution. Actually, as a preferable alternative, one can reformulate the problem so that upper and lower bounds on the true solution and not the true solution itself would have to

be sought. Such a reformulation can be based on Levine and Schwinger's result that when the aperture is electrically small there is a variational principle for the upper bound and another variational principle for the lower bound [7, 8]. However, this variational approach, which was used by Fikhmanas and Fridberg to find bounds on the electric and magnetic polarizabilities of electrically small apertures [9], does not lend itself to very easy calculation. Accordingly, it is of some interest to try a simpler method of sandwiching the true solution between upper and lower bounds.

In this paper we shall examine how symmetrization, which has yielded interesting results in geometry and mathematical physics [10], may be used to establish two-sided bounds on the electric and magnetic polarizabilities of differently shaped convex apertures and thereby estimate their transmission properties in a simple economical manner.

1. Symmetrization

Of the several kinds of symmetrization that have been invented we shall restrict our attention to the symmetrization of a plane figure with respect to a straight line. To symmetrize a plane figure with respect to a straight line L , we suppose the figure to consist of line segments that are parallel to each other and perpendicular to L (see Fig. 1). We then shift each line segment along its own line until the line segment is bisected by L . The shifted line segments compose the symmetrized figure. For example, a semicircle of radius R , when symmetrized with respect to its bounding

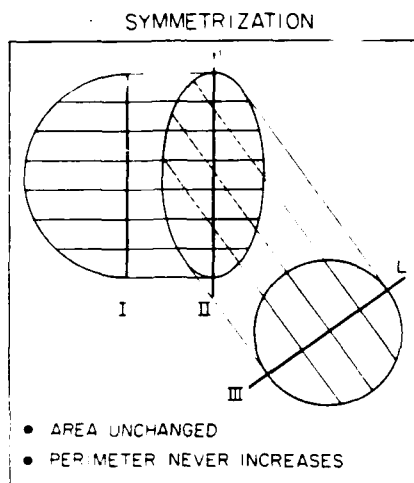


Fig. 1. Example of symmetrization of a plane figure with respect to a line L . The semi-circle of radius R is symmetrized with respect to its bounding diameter to produce an ellipse with semi-axes R and $R/2$. The ellipse, when symmetrized, becomes a circle of radius $R/2$. The area of each figure remains constant but the perimeter decreases with each symmetrization.

diameter, changes into an ellipse with semi-axes R and $R/2$. A further symmetrization can transform the ellipse into a circle of radius $R/2$. Symmetrization leaves the figure's area A unchanged and decreases, or, more accurately, never increases its perimeter P . For the case shown in Fig. 1, the area is always $\pi R^2/2$ and the perimeter varies from $(2+\pi)R$ for the semicircle to $2^{1/2}\pi R$ for the circle.

As an instructive example, we apply the principle of symmetrization to the calculation of capacitance C . It is known that the symmetrization of a plane conducting plate decreases (i.e., never increases) the electrostatic capacity of the plate [10]. A plane figure symmetrized infinitely many times becomes a circle and, consequently, of all conducting plates of a given area the circular plate has the minimum capacity. Accordingly,

$$C \geq C_{in} \quad (1)$$

where C denotes the electrostatic capacitance of a plane conducting plate and C_{in} denotes the electrostatic capacitance of the circular plate of radius r_{in} , that has been obtained by completely symmetrizing the original plate. This places a lower bound on C . To obtain an upper bound, we invoke the conjecture that of all plates with a given perimeter, the circular plate has the maximum capacitance [10]. Thus we find

$$C_{out} \geq C \quad (2)$$

where C_{out} is the electrostatic capacitance of a circular plate of radius r_{out} , whose perimeter is equal to that of

the perimeter of the original plate. From (1) and (2) it follows that

$$C_{in} \leq C \leq C_{out} \quad (3)$$

Since we have

$$r_{in} = (A/\pi)^{1/2} \quad (4)$$

$$r_{out} = P/2\pi \quad (5)$$

and the electrostatic capacitance of a circular plate (disk) in MKS units is given by

$$C = 8\epsilon_0 a, \quad (6)$$

where a is the radius of the disk and ϵ_0 is the dielectric constant of free space, upon replacing a by r_{in} and r_{out} we obtain from (3)–(6) that the capacitance C of a plate of area A and perimeter P is delimited by

$$(A/\pi)^{1/2} \leq C/8\epsilon_0 \leq P/2\pi \quad (7)$$

Here $\epsilon_0 = (36\pi)^{-1} \times 10^{-9}$ farads per meter.

Both Maxwell [11] and Rayleigh [12] made unproven statements concerning bounds on the capacitance of plates, which agree with (7). Moreover, the capacitance of an elliptic plate of eccentricity e , as given by

$$C_{\text{ellipse}} = 8\epsilon_0 (A/\pi)^{1/2} (1-e^2)^{-1/4} / 2K(e^2) \xrightarrow{e \rightarrow 0} (A/\pi)^{1/2} (1+e^2/64), \quad (8)$$

where $K(e^2)$ is the complete elliptic integral of the first kind [12], clearly satisfies the left side of (7). To show that it also satisfies the right side we only need to recall that for an ellipse

$$P_{\text{ellipse}} = 2\pi (A/\pi)^{1/2} E(e^2) (1-e^2)^{-1/4} \xrightarrow{e \rightarrow 0} (A/\pi)^{1/2} (1+3e^2/64), \quad (9)$$

where $E(e^2)$ is the complete elliptic integral of the second kind.

By virtue of the apparent validity of (7) for the capacitance of plates of arbitrary size and shape we are led to believe that other quantities of physical interest may be similarly sandwiched between bounds involving only the purely geometric parameters A and P .

2. Polarizabilities and Transmission Coefficients of Small Apertures

Let us now consider the transmission of electromagnetic energy through an electrically small aperture which is located in a plane screen of perfect conductivity and zero thickness. Since the aperture is small, the fields on the shadow side of the screen appear to emanate from dipoles located in the aperture. These electric and magnetic dipoles, having moments \mathbf{p} and \mathbf{m} ,

radiate in free space and are linearly related to the incident traveling wave through the vector electric polarizability with components α_i and the dyadic magnetic polarizability with components β_{ij} . That is,

$$P_i = \epsilon_0 \alpha_i E_i^{\text{inc}} \quad (i = 1, 2, 3) \quad (10)$$

$$-m_i = \mu_0 \sum_{j=1}^3 \beta_{ij} H_j^{\text{inc}} \quad (i = 1, 2) \quad (11)$$

where $\mu_0 = 4\pi \times 10^{-7}$ henries per meter. The incident electric and magnetic fields are plane waves of the form $E^{\text{inc}} \exp[i(\mathbf{k} \cdot \mathbf{r} - \omega t)]$ and $H^{\text{inc}} \exp[i(\mathbf{k} \cdot \mathbf{r} - \omega t)]$, where \mathbf{r} is the position vector, \mathbf{k} is the wave vector and ω is the frequency. We emphasize here that "electrically small" means that $kL \ll 1$ where L is the maximum linear dimension of the aperture.

For a circular aperture of radius a the polarizabilities are given by the simple expressions

$$\alpha_i^{\text{circle}} = \frac{8}{3} a^3 \delta_{i3} \quad (i = 1, 2, 3) \quad (12)$$

$$\beta_{ij}^{\text{circle}} = \frac{16}{3} a^3 \delta_{ij} \quad (i, j = 1, 2) \quad (13)$$

where

$$\delta_{ij} = \begin{cases} 1 & i=j \\ 0 & i \neq j. \end{cases}$$

The values 1, 2, and 3 correspond respectively to the directions \hat{e}_1 , \hat{e}_2 , and \hat{e}_n . The aperture plane is defined by the unit vectors \hat{e}_1 and \hat{e}_2 and the normal (pointing toward the shadow side) is defined by $\hat{e}_n = \hat{e}_1 \times \hat{e}_2$ (see Fig. 2). The polarizabilities are defined here for incident traveling waves and for dipoles radiating in free space. For short circuit incident fields and for dipoles radiating in the presence of a conducting wall, all values of the polarizabilities should be divided by the numeric 4.

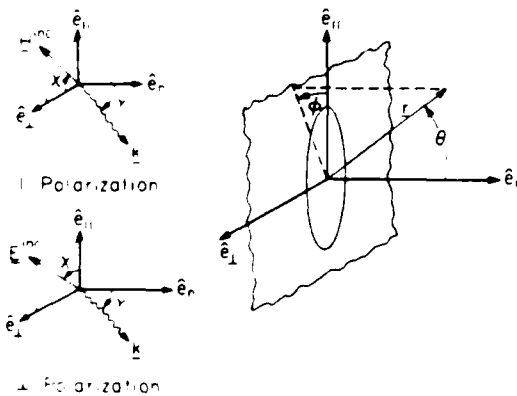


Fig. 2 Unit vectors \hat{e}_1 and \hat{e}_2 lie in the aperture plane, and \hat{e}_n is normal to the aperture plane. For parallel polarization H^{inc} is always parallel to the aperture plane and makes angle γ with respect to \hat{e}_1 . For perpendicular polarization E^{inc} is always parallel to the aperture plane and makes angle χ with respect to \hat{e}_1 .

For elliptic apertures with semi-axes a and b along \hat{e}_1 and \hat{e}_2 , respectively, we have

$$\alpha_i^{\text{ellipse}} = \frac{4\pi}{3} \frac{ab^2}{E(e^2)} \delta_{i3} \quad (14)$$

$$\beta_{ij}^{\text{ellipse}} = \begin{cases} \frac{4\pi}{3} \frac{ab^2 e^2}{(1-e^2)[K(e^2) - E(e^2)]} \delta_{i1} \\ \frac{4\pi}{3} \frac{ab^2 e^2}{E(e^2) - (1-e^2)K(e^2)} \delta_{i2} \end{cases} \quad (15)$$

$$(16)$$

where $e = (1 - b^2/a^2)^{1/2}$ is the eccentricity of the ellipse and $K(e^2)$ and $E(e^2)$ are elliptic integrals of the first and second kind [13].

The transmission coefficient τ is defined as the ratio of the total far-field power transmitted through the aperture divided by the total power incident on the aperture. For the case where the principal axes of magnetic polarizability dyadic correspond to \hat{e}_1 and \hat{e}_2 , we find

$$\tau = \frac{k^4}{12\pi A} \left[\alpha_3^2 \sin^2 \gamma \begin{pmatrix} 0 \\ 1 \end{pmatrix} + (\beta_{11}^2 \sin^2 \chi + \beta_{22}^2 \cos^2 \chi) \begin{pmatrix} \cos^2 \gamma \\ 1 \end{pmatrix} \right] \quad (17)$$

for $\begin{pmatrix} 1 \\ 0 \end{pmatrix}$ polarization [14]. Here γ is the angle of incidence, i.e. the angle between \mathbf{k} and \hat{e}_n , and χ is the angle between H^{inc} and \hat{e}_1 for parallel polarization and is the angle between E^{inc} and \hat{e}_1 for perpendicular polarization (see Fig. 2).

3. Bounds on Polarizabilities and Transmission Coefficient

Imitating the procedure we followed to establish bounds on the capacitance of plates, we now construct bounds on the mean magnetic polarizability β_m of a convex aperture by replacing the radius a , which appears in expression (13) for the polarizability of a circular aperture, by r_{in} (4) and r_{out} (5) of the aperture. Thus we are led to the conjecture

$$\frac{16}{3} \left(\frac{A}{\pi} \right)^{3/2} \leq \beta_m \leq \frac{16}{3} \left(\frac{P}{2\pi} \right)^3 \quad (18)$$

where by definition $\beta_m = (\beta_{11} + \beta_{22})/2$.

To test the plausibility of (18) we examine several special cases. For the elliptic aperture of small eccentricity ($e \ll 1$), (18) becomes

$$\frac{16}{3} \left(\frac{A}{\pi} \right)^{3/2} \leq \beta_m \leq \frac{16}{3} \left(\frac{A}{\pi} \right)^{3/2} \left(1 + \frac{9}{64} e^4 \right) \quad (19)$$

(15) and (16) yield

$$\beta_m = \frac{16}{3} \left(\frac{A}{\pi} \right)^{3/2} \left(1 + \frac{3}{32} e^4 \right) \quad (20)$$

and thus we clearly see that (18) is satisfied in the case of mildly eccentric ellipses. It can also be shown that (18) holds true for elliptic apertures of arbitrary eccentricity ($0 \leq e \leq 1$) and for other convex apertures such as the rectangular and the rhombical aperture [14, 15]. The fact that these test cases are in complete agreement with (18) leads us to believe that the assertion (18) is valid for all convex apertures.

Accepting the general validity of (18) and recalling that symmetrization reduces P without changing A we conclude that of all convex apertures of fixed area A the circular aperture possesses the smallest mean magnetic polarizability.

The electric polarizability contributes to transmission through small apertures only when the incident wave is obliquely incident and polarized parallel to the plane of incidence. To construct bounds for the electric polarizability we note that, for a circular aperture of radius a and area A , (12) can be written as

$$\alpha_i^{\text{circle}} = \frac{8}{3\pi^2} \frac{A^2}{a} \delta_{i3}. \quad (21)$$

Then by replacing the radius a of this expression by r_{in} (4) and r_{out} (5) we arrive at the conjecture

$$\frac{16}{3\pi} \frac{A^2}{P} \leq \alpha_3 \leq \frac{8}{3} \left(\frac{A}{\pi} \right)^{3/2}. \quad (22)$$

To test the plausibility of (22) we again consider the case of a mildly eccentric ellipse ($e \ll 1$). In this case (22) becomes

$$\frac{8}{3} \left(\frac{A}{\pi} \right)^{3/2} \left(1 - \frac{3}{64} e^4 \right) \leq \alpha_3^{\text{ellipse}} \leq \frac{8}{3} \left(\frac{A}{\pi} \right)^{3/2} \quad (23)$$

and from (14) we have

$$\alpha_3^{\text{ellipse}} = \frac{8}{3} \left(\frac{A}{\pi} \right)^{3/2} \left(1 - \frac{3}{64} e^4 \right). \quad (24)$$

Obviously, expression (24) is equal to the lower bound in (23). Furthermore, with the aid of (14) it can be verified that the lower bound in (22) is precisely the value of the electric polarizability of ellipses of arbitrary eccentricity [9, 15]. Also we note that the electrical polarizabilities of rectangular and rhombical apertures satisfy (22) [14, 15].

Assuming the validity of (22) and invoking symmetrization, we find that of all convex apertures of fixed area the circular aperture possesses the largest electric polarizability.

The bounds that have been proposed for the electric (22) and mean magnetic (18) polarizabilities can be used to obtain bounds on the transmission coefficient (17). In some modern applications the quantity of interest is the upper bound for the case where the incident wave is

directed and polarized to maximize the transmission through the given aperture. Clearly, maximum possible transmission through a given aperture occurs when the incident wave is parallel polarized and is made to fall on the aperture at grazing incidence. To find the upper bound for maximum possible transmission we use (22) and note that $r_{\text{out}} \geq r_{\text{in}}$. Thus

$$\alpha_3^2 \sin^2 \chi \leq \frac{64}{9} \left(\frac{A}{\pi} \right)^3 \leq \frac{64}{9} \left(\frac{P}{2\pi} \right)^6. \quad (25)$$

Moreover, in view of (18) we can write

$$\beta_{11}^2 \sin^2 \chi + \beta_{22}^2 \cos^2 \chi \leq \frac{1024}{9} \left(\frac{P}{2\pi} \right)^6. \quad (26)$$

Substituting (25) and (26) into (17) we thus obtain the following expression for the maximum possible transmission through a small aperture of area A and perimeter P

$$\tau \leq \frac{68(P/\lambda)^6}{27\pi^3(A/\lambda^2)}. \quad (27)$$

where $\lambda = 2\pi k$ is the wavelength of the incident radiation.

Since symmetrization reduces P and keeps A unchanged we see from (27) that the maximum possible transmission decreases as the aperture is symmetrized. That is, the maximum possible transmission decreases as the shape of the aperture approaches that of a circle [16].

Conclusions

We suggest bounds for the polarizabilities of a small convex aperture of arbitrary shape and given area and thus find plausible upper and lower bounds on its transmission coefficient. Symmetrizing the aperture we see that the aperture's perimeter decreases and accordingly the maximum possible transmission decreases as the shape of the aperture approaches that of a circle. For example, the maximum possible transmission decreases as the shape of the aperture is changed from that of an equilateral triangle to that of a square and finally to that of a circle.

The bounds are simple to evaluate from a knowledge of the aperture's area and perimeter and therein lies the desirability and economy of this method.

It appears that this method of estimation can be generalized to handle other boundary-value problems and thus provide information as to how their solutions are modified when there is a change of shape.

Acknowledgement. The authors are greatly indebted to Dr. K. S. H. Lee for his valuable assistance. This work was supported by the Dikewood Corporation and the U.S. Air Force Office of Scientific Research under Grant No. AFOSR-77-3451.

References

1. L.W. Ricketts, J.E. Bridges, J. Miletta: *EMP Radiation and Protective Techniques* (John Wiley and Sons, New York 1976)
2. Lord Rayleigh: "On the passage of Waves through Apertures in Plane Screens, and Allied Problems". *Phil. Mag.* XLIII, 259—272 (1897); also "On the Incidence of Aerial and Electric Waves upon Small Obstacles in the Form of Ellipsoids or Elliptic Cylinders, and on the Passage of Electric Waves through a Circular Aperture in a Conducting Screen". *Phil. Mag.* XLIV, 28—52 (1897)
3. H.A. Bethe: "Theory of Diffraction by Small Holes". *Phys. Rev.* 60, 163—182 (1942)
4. C.J. Bouwkamp: "On Bethe's Theory of Diffraction by Small Holes". *Philips Res. Rep.* 5, 321—332 (1950); also "On the Diffraction of Electromagnetic Waves by Small Circular Disks and Holes". *Philips Res. Rep.* 5, 401—422 (1950)
5. J. Meixner, W. Andrejewski: "Strenge Theorie der Beugung ebener elektromagnetischer Wellen der vollkommen leitenden ebenen Schirme". *Ann. Phys.* 7, 157—168 (1950)
6. W. Andrejewski: "Die Beugung elektromagnetischer Wellen an der leitenden Kreisscheibe und der kreisförmigen Öffnung in leitenden ebenen Schirmen". *Z. Angew. Phys.* 5, 178—186 (1953)
7. H. Levine, J. Schwinger: "On the Theory of Electromagnetic Wave Diffraction by an Aperture in an Infinite Plane Conducting Screen". *Commun. Pure Appl. Math.* 3, 355—391 (1950)
8. F.E. Borgnis, C.H. Papas: *Randwertprobleme der Mikrowellenphysik* (Springer, Berlin 1955)
9. R. Fikhrmanas, P. Fridberg: "Variational Estimate of Upper and Lower Bounds on the Coefficient of Polarizability in the Theory of Pinhole Diffraction". *Sov. Phys.-Doklady* 14, 1155—1157 (1970); also "Theory of Diffraction at Small Apertures. Computation of Upper and Lower Boundaries of the Polarizability Coefficients". *Radio Eng. Electron. Phys.* 18, 824—829 (1973)
10. G. Pólya, G. Szegő: *Isoperimetric Inequalities in Mathematical Physics* (Princeton Univ. Press, Princeton 1951); also "Inequalities for the Capacity of a Condenser". *Amer. J. Math.* 67, 1—32 (1945); L.E. Payne: "Isoperimetric Inequalities and their Application". *SIAM Review* 9, 453—487 (1967)
11. J. Maxwell (Ed.): *The Scientific Papers of the Honorable Henry Cavendish*, Vol. 1 (1897), reprinted by Cambridge Univ. Press, Cambridge (1921)
12. Lord Rayleigh: *The Theory of Sound*, Vol. 2 (1896), reprinted by Dover New York (1945)
13. See, for example, C. Montgomery, R. Dicke, E. Purcell: *Principles of Microwave Circuits* (McGraw Hill, New York 1948) or R. Collin: *Field Theory of Guided Waves* (McGraw Hill, New York 1960)
14. D.L. Jaggard: "Transmission Through One or More Small Apertures of Arbitrary Shape". *Calif. Inst. Tech. Antenna Lab. Tech. Rept. No. 83*, Calif. Inst. of Tech. (May 1977)
15. R. Latham: "Small Holes in Cable Shields". *EMP Interaction Note* 118 (Sept. 1972)
16. C.H. Papas: "An Application of Symmetrization to an EMP Shielding Problem". *Calif. Inst. Tech. Ant. Lab. Tech. Rept. No. 80*, Calif. Inst. of Tech. (Dec. 1976)

On Electromagnetic Waves in Chiral Media

D. L. Jaggard*, A. R. Mickelson, and C. H. Papas

Division of Engineering and Applied Science, California Institute of Technology, Pasadena, CA 91125, USA

Received 1 August 1978 Accepted 21 August 1978

Abstract. We analyze the propagation of electromagnetic waves through chiral media, i.e., through composite media consisting of macroscopic chiral objects randomly embedded in a dielectric. The peculiar effects that such media have on the polarization properties of the waves are placed in evidence. To demonstrate the physical basis of these effects, a specific example, chosen for its analytical simplicity, is worked out from first principles.

PACS: 02.41

Chirality is quite common. It occurs not only in nature but also in works of art and architecture as well as in manufactured articles [1, 2]. In nature we find chirality on a molar scale in, for example, snails, flowers, and vines, and on a molecular scale in such substances as grape sugar and fruit sugar. Moreover, chirality is an operational feature of such manufactured articles as screws, springs, and golf clubs.

Since chirality begets handedness and handedness begets optical activity, it is not surprising that the interaction between an electromagnetic wave and a collection of randomly oriented chiral objects can be such as to rotate the plane of polarization of the wave to the right or to the left depending on the handedness of the objects.

The concept of chirality is not new, nor has it been ignored. Since the early part of the nineteenth century, it has played an increasingly important role in chemistry [3–5], optics [6, 7], and elementary particle physics [8]. In 1811 Arago [9] discovered that crystals of quartz rotate the plane of polarization of plane polarized light and hence are optically active. Shortly thereafter, circa 1815, Biot [10] discovered that this optical activity is not restricted to crystalline solids but appears as well in other media such as oil of turpentine and aqueous solutions of tartaric acid. These discoveries led to the fundamental problem of determining the basic cause of optical activity. In 1848 Louis Pasteur [3] solved the problem by postulating that the

optical activity of a medium is caused by the chirality of its molecules. Thus, Pasteur introduced geometry into chemistry and originated the branch of chemistry we now call stereochemistry. More recently, in 1920 and 1922, Lindman [11, 12] devised a macroscopic (molar) model for the phenomenon by using microwaves instead of light, and wire spirals instead of chiral molecules. The validity of the model was verified a few years later by Pickering [13].

To obtain a better understanding of chirality and assay its future role in electrical design, we shall examine in the following pages the interaction between electromagnetic waves and chiral objects. In particular, we shall study the case of a composite medium consisting of randomly oriented chiral conductors embedded in a dielectric.

1. Two Conjectures on Chiral Objects

Chirality is a purely geometric notion which refers to the lack of symmetry of an object. By definition, an object is chiral if it cannot be brought into congruence with its mirror image by translation and rotation. An object that is not chiral is said to be achiral. Thus all objects are either chiral or achiral. Some chiral objects occur naturally in two versions related to each other as a chiral object and its mirror image. Objects so related are said to be enantiomorphs of each other.

A chiral object has the property of handedness: it must be either left-handed or right-handed. If a chiral object is left-(right-)handed, its enantiomorph is right-(left-)

* Presently with the Department of Electrical Engineering, University of Utah, Salt Lake City, Utah 84112, USA

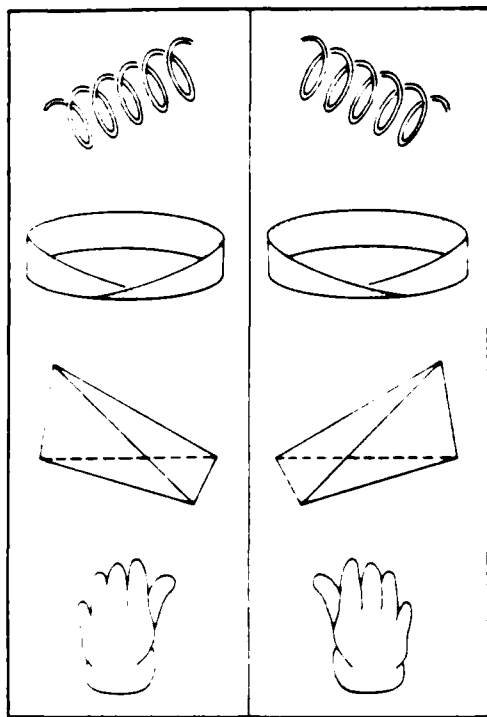


Fig. 1 A sketch showing chiral objects (left column) and their enantiomorphs (right column). From top to bottom are shown a helix, a Möbius strip, an irregular tetrahedron and a glove.

handed. For example, if the chiral object is a left-(right-handed) helix, its enantiomorph is a right-(left-handed) helix.

The handedness of helices was made clear by Lindman's and Pickering's experimental results which showed that a collection of randomly oriented left-handed helices would rotate the plane of polarization of a linearly polarized microwave one way but that a collection of randomly oriented right-handed helices would rotate the plane of polarization the opposite way.

Assuming that this relation between the handedness of the helices and the sense of rotation of the microwave is not peculiar only to helices but is a property of all chiral objects and their enantiomorphs, we are led to the following conjecture: Any medium composed of randomly oriented equivalent (simply-connected) chiral objects will rotate the plane of polarization one way, say, to the left, while a medium composed of the enantiomorphs of these objects will rotate the plane of polarization the opposite way, i.e., to the right.

In Fig. 1 we see common examples of chiral objects: a helix, a Möbius strip, an irregular tetrahedron, and a

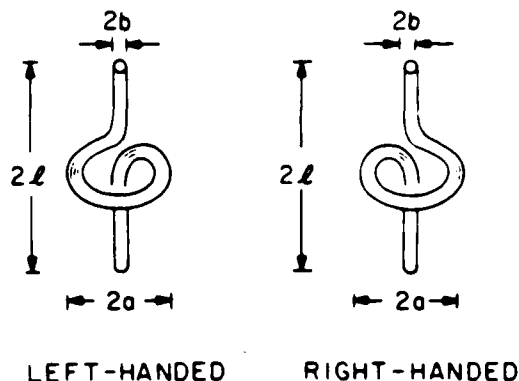


Fig. 2 Idealized short helices used in calculations. The plane of the loop is perpendicular to the axis of the straight portion of the wire.

glove. On one side of the figure is the chiral object and on the other is its enantiomorph.

A type of (multiply-connected) chiral object that has recently attracted considerable attention is the wire braid. The theory of braids is a developing branch of topology [14, 15] and a study of how an electromagnetic wave interacts with a braid may help in the development of the theory.

Examining the forces that are exerted on certain simple chiral configurations of wire when an electromagnetic wave falls on them, we conjecture that the forces are such as to reduce the chirality of the configurations. This is true for the wire helix, for the three-stranded braid, and appears to be true in general. This tendency of the forces makes the object more nearly symmetrical.

2. The Short Helix

To demonstrate the plausibility of the above conjectures, we examine the scattering of electromagnetic waves from a metallic chiral object. For computational simplicity, the chiral object is chosen to be an electrically small perfect conductor having the form of a short right- or left-handed helix, as shown in Fig. 2. The calculation is simplified by referring the incident and scattered waves to the scattering plane defined by the incident and scattered wave vectors $\mathbf{k}' = k\hat{e}_\theta$ and $\mathbf{k} = k\hat{e}_\phi$, respectively (Fig. 3). The incident plane wave is composed of the electric field

$$\mathbf{E}' = (a_{||}\hat{e}'_{||} + a_{\perp}\hat{e}'_{\perp})e^{i\mathbf{k}'\cdot\mathbf{r}} \quad (1)$$

and the corresponding magnetic field

$$\mathbf{B}' = \hat{e}'_{\perp} \times \mathbf{E}'/c, \quad (2)$$

where c is the free-space speed of light, $a_{||}$, a_{\perp} , and δ are real numbers with $a_{||}^2 + a_{\perp}^2 = 1$, and z is the distance along $\hat{e}'_n (= \hat{e}'_{||} \times \hat{e}'_{\perp})$. The circumflexed quantities are unit vectors, the primes denote quantities associated with the incident wave, and the subscripts identify quantities parallel or perpendicular to the scattering plane. The harmonic time dependence $\exp(-i\omega t)$ (where $\omega = ck$) has been suppressed.

The scattered electric field $E_s(\theta)$ depends on the observation angle θ , defined by the relation $\cos \theta = \hat{e}'_n \cdot \hat{e}_n$, and on the induced electric and magnetic dipole moments \mathbf{p} and \mathbf{m} . It is apparent (Fig. 2) that both dipole moments are directed parallel to the axis of the helix. This axis lies along the unit vector \hat{e}_d whose orientation angles are α and β (Fig. 3).

The incident electric field induces currents in the straight portion of the chiral object, and by continuity these currents must also flow in the circular portion of the object. The current in the straight portion contributes to the electric dipole moment of the object and the current in the circular portion contributes to its magnetic dipole moment. In a complementary manner, the incident magnetic field induces currents in the circular portion and by continuity in the straight portions. Thus, also the magnetic field contributes to the electric and magnetic dipole moments of the object. In a first-order (Born) approximation we find from the heuristic argument above that the electric and magnetic dipole moments of the object are given by

$$\mathbf{p} = i\omega [\chi_e(\hat{e}_d \cdot \mathbf{E}) \pm i\chi_{em}c(\hat{e}_d \cdot \mathbf{B})]\hat{e}_d \quad (3)$$

$$\mathbf{m} = \eta^{-1} [-\chi_m c(\hat{e}_d \cdot \mathbf{B}) \mp i\chi_{me}(\hat{e}_d \cdot \mathbf{E})]\hat{e}_d \quad (4)$$

Here, as in the remainder of the report, the upper (lower) sign corresponds to the right-handed (left-handed) helix of Fig. 2. The permittivity, the permeability, and the impedance of free space are denoted by ϵ_0 , μ_0 , $\eta = (\mu_0/\epsilon_0)^{1/2}$. The electric and magnetic self-susceptibilities, χ_e and χ_m , are real positive quantities as are the cross-susceptibilities χ_{em} and χ_{me} . Clearly, χ_e and χ_m are the usual electric and magnetic susceptibilities associated with electrically small metallic bodies. The cross-susceptibilities χ_{em} and χ_{me} are, in a certain sense, a measure of chirality or handedness since for achiral bodies $\chi_{em} = \chi_{me} = 0$.

Using known approximations, the self-susceptibilities can be written

$$\chi_e = (2l)^2 C/\epsilon_0 \quad (5)$$

$$\chi_m = (\pi a^2)^2 \mu_0/L \quad (6)$$

where C and L are, respectively, the capacitance and the inductance of the body [16], and $2l$ and $2a$ represent the length and the width of the short helix (Fig. 2). It can be shown that the cross-susceptibilities

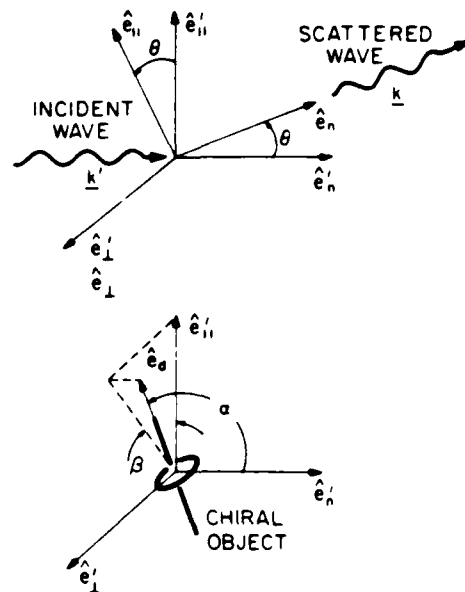


Fig. 3 Vectors indicating the directions and angles of incident and scattered waves and the orientation angles of the chiral object. The axes are oriented in such a manner that the unit vectors \hat{e}'_n , \hat{e}_n , and \hat{e}_d are in the scattering plane defined by \mathbf{k} and \mathbf{k}' . The unit vectors \hat{e}'_{\perp} and \hat{e}_{\perp} are perpendicular to this plane.

are given by

$$\chi_{em} = \chi_m(2l/\pi a^2 k) \quad (7)$$

$$\chi_{me} = \chi_e(\pi a^2 k/2l) \quad (8)$$

From physical considerations (i.e., freedom from ohmic losses and conservation of energy), it appears that χ_{em} and χ_{me} are equal and real, i.e.,

$$\chi_{em} = \chi_{me} = \chi_c \quad (9)$$

where χ_c is their real common value.

It follows from (5)-(9) that the constraint

$$LC = \epsilon_0^{-2} \quad (10)$$

is placed upon the inductance and capacitance of the helix and the common value χ_c for the cross-susceptibilities is related to the inductance and capacitance by

$$\chi_c = 2l\pi a^2 \eta \omega L = 2l\pi a^2 \eta \omega C \quad (11)$$

From the knowledge of \mathbf{p} and \mathbf{m} the scattered field can be calculated by the formula

$$\mathbf{E}_s(\theta) = \frac{k^2 e^{ikr}}{4\pi\epsilon_0 r} [(\hat{e}_n \times \mathbf{p}) \times \hat{e}_n - \hat{e}_n \times \mathbf{m} \times \hat{e}_n] \quad (12)$$

To gain further insight into the problem, it is useful to find the constitutive relations of a medium composed

of randomly oriented equivalent chiral objects. These constitutive relations must have the form [17]

$$\mathbf{P} = \gamma_e \mathbf{E} + \gamma_{em} \mathbf{B} \quad (13)$$

$$\mathbf{M} = \gamma_{me} \mathbf{E} + \gamma_m \mathbf{B}, \quad (14)$$

where \mathbf{P} and \mathbf{M} are, respectively, the polarization and magnetization of the medium.

Energy conservation dictates that for a lossless medium

$$\gamma_{me} = \gamma_{em}^*, \quad (15)$$

where the asterisk denotes complex conjugate. If γ_{me} and γ_{em} not only satisfy (15) but also are purely imaginary quantities, then the constitutive relations (13) and (14) are those of an optically active medium [17].

To find the constitutive parameters for a medium composed of N non-interacting short helices per unit volume, we compare (3) and (4), averaged over orientation angles α and β , with (13) and (14). Thus we obtain

$$\gamma_e = N\epsilon_0\chi_e/4 \quad (16)$$

$$\gamma_m = -N\chi_m/4\mu_0 \quad (17)$$

$$\gamma_{em} = \pm iN\chi_{em}/4\eta \quad (18)$$

$$\gamma_{me} = \mp iN\chi_{me}/4\eta \quad (19)$$

Since χ_{em} and χ_{me} are real and equal, we see from (18) and (19) that γ_{me} and γ_{em} are purely imaginary and satisfy (15). Hence the medium composed of short helices exhibits optical activity.

3. Collection of Short Helices

To find the scattered field of a collection of randomly oriented identical helices we can use one of two approaches. One approach uses (12) averaged over orientation angles α and β ; the other approach uses (13) and (14) directly. These two approaches give the same result. Here we use the former of the two approaches.

Let us suppose that we have a collection of N non-interacting helices per unit volume occupying a small volume ΔV . When the incident wave is circularly polarized, the scattering cross-sections per unit solid angle Ω are found to be

$$\left(\frac{d\sigma(\theta)}{d\Omega}\right)_{\text{RCP-RCP}} = \frac{(k^2 N \Delta V)^2}{1024\pi^2} |\chi_e - \chi_m \pm 2\chi_c|^2 (1 + \cos \theta)^2 \quad (20)$$

when the incident wave is right circularly polarized (RCP) and only the right circularly polarized part of

the scattered field is considered.

$$\left(\frac{d\sigma(\theta)}{d\Omega}\right)_{\text{LCP-LCP}} = \frac{(k^2 N \Delta V)^2}{1024\pi^2} |\chi_e - \chi_m \mp 2\chi_c|^2 (1 + \cos \theta)^2 \quad (21)$$

when the incident wave is left circularly polarized (LCP) and only the left circularly polarized part of the scattered field is considered, and

$$\begin{aligned} \left(\frac{d\sigma(\theta)}{d\Omega}\right)_{\text{RCP-LCP}} &= \left(\frac{d\sigma(\theta)}{d\Omega}\right)_{\text{LCP-RCP}} \\ &= \frac{(k^2 N \Delta V)^2}{1024\pi^2} |\chi_e + \chi_m|^2 (1 - \cos \theta)^2 \end{aligned} \quad (22)$$

when the incident wave is RCP or LCP and the scattered field is LCP or RCP, respectively.

From these expressions we see that for scattering in the forward direction ($\theta=0$) right (left) circular polarization produces a right (left) circularly polarized scattered field whereas in the backward direction ($\theta=\pi$) right (left) circular polarization produces a left (right) circularly polarized scattered field.

Next, we consider a wave normally incident on an electrically thin slab of width d which contains N randomly oriented helices per unit volume. Using again the assumption that the helices are non-interacting, we find from averaging (12) that the transmitted field is given by

$$\begin{aligned} \mathbf{E}_{tr} \approx & \left\{ a_{\parallel} \hat{e}_{\parallel} + a_{\perp} e^{i\phi} \hat{e}_{\perp} \right. \\ & + \frac{iNkd}{8} \left\{ [a_{\parallel}(\chi_e - \chi_m) \mp ia_{\perp} e^{i\phi} 2\chi_c] \hat{e}_{\parallel} \right. \\ & \left. \left. + i[\pm a_{\parallel} 2\chi_c - ia_{\perp} e^{i\phi}(\chi_e - \chi_m)] \hat{e}_{\perp} \right\} \right\} e^{ikz} \end{aligned}$$

and the reflected field by

$$\mathbf{E}_{ref} \approx \frac{iNkd}{8} (\chi_e + \chi_m) [a_{\parallel} \hat{e}_{\parallel} + a_{\perp} e^{i\phi} \hat{e}_{\perp}] e^{-ikz} \quad (24)$$

where the above expressions are correct to the first order in $(Nkd\chi)$ (here χ stands for χ_e , χ_m or χ_c). From (23) it can be shown that the plane of polarization is rotated through the angle ϕ where

$$\phi \approx \tan \phi = \mp Nkd\chi_c/4 \quad (25)$$

for waves which pass through the chiral medium. Here ϕ is measured from \hat{e}_{\parallel} towards \hat{e}_{\perp} . Expression (25) is again correct to the first order in $(Nkd\chi)$. This equation expresses a general result which holds for any medium composed of objects characterized by parallel electric and magnetic dipole moments with non-zero cross-susceptibilities. For the short helices pictured in Fig. 2 we can find a lower bound on the capacitance C by the

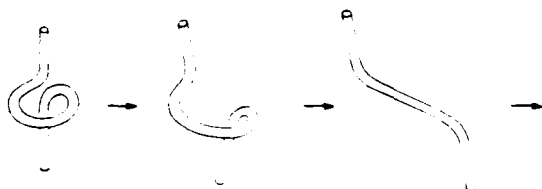


Fig. 4 A schematic of a short helix (chiral) evolving into a straight wire (achiral) under the influence of forces produced by induced currents

expression [18]

$$C \geq \epsilon_0 (4\pi)^2 (3V_h)^{1/3} \quad (26)$$

where $V_h (= 2\pi b^2(l + \pi a))$ is the volume occupied by the short wire helix and b is the wire radius. This inequality, with the aid of (11) and (25), yields the following lower bound for the magnitude of the rotation angle

$$|\phi| \geq |\tan \phi| \geq 4^{-1/3} \pi^2 N(kd)(2l)(\pi a^2)(3k^3 V_h)^{1/3}. \quad (27)$$

This bound is proportional to the product of the third root of the volume V_h of the wire helix and the cylindrical volume containing the helix ($= 2l\pi a^2$).

From (23) the eccentricity of the transmitted polarization ellipse differs from that of the incident polarization ellipse by a factor of order $(Nkd\chi)^2$. However, this transmitted field is correct only to order $(Nkd\chi)$. Therefore, the change in the eccentricity of the polarization ellipse cannot be determined exactly from this model. To the first order in $(Nkd\chi)$ the eccentricity is unchanged.

The reflected wave (24) to order $(Nkd\chi)$ shows zero rotation for the plane of polarization and zero change in the eccentricity for the polarization ellipse. Therefore, for reflected waves, the slab of chiral medium behaves as an ordinary dielectric slab. These polarization characteristics are due to the fact that in the backscatter direction, in the first order, the effects of chirality are not present in the scattered field [see (20), (21), and (23)].

From Noether's theorem [19] it can be shown that the angular momentum of the electromagnetic field is conserved for a medium described by (13)–(19). This implies that no torque is exerted on a slab of chiral medium. It is not surprising that there is no torque since the electrical properties of the slab are invariant under rotations of the slab about \hat{e}_z . With a knowledge of the state of polarization of the incident wave, conservation of field angular momentum further implies that the state of polarization of the reflected wave can be determined from the state of polarization of the transmitted wave, and vice versa. Some experimental

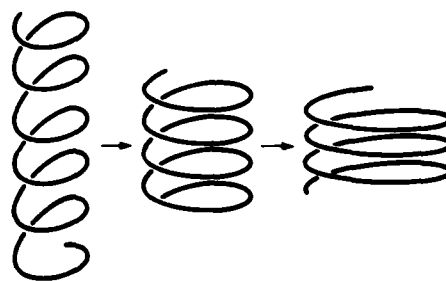


Fig. 5 Under the action of forces produced by the induced currents a long helix (shown at left) is gradually shortened into more closely spaced loops of increased radius (shown at right)

results indicate that there is a change of eccentricity between the incident and scattered fields due to the chiral medium [11, 12].

From the above considerations, the conjecture that a collection of chiral objects will rotate the plane of polarization becomes plausible.

4. Reduction of Chirality

Assuming that the helix in Fig. 4 is made of flexible wire, we see that the currents that are induced tend to deform the helix. The current along the circular portion tends to open up the circle and make a planar figure out of the original helix. Moreover, interaction with the current along the straight portion of the helix tends to elongate the planar figure into a straight line. Since planar figures are achiral, we thus see that the helix evolves into a planar figure and that the chirality of the configuration is reduced.

Suppose now that we have a flexible helix of many turns (Fig. 5). In this case the induced current forces adjacent turns together and at the same time makes each turn expand into a turn of larger radius. Thus the original helix becomes a shortened helix of larger radius. Since the shortened helix is less chiral than the original helix, we see that here again the induced currents tend to reduce the chirality of the configuration.

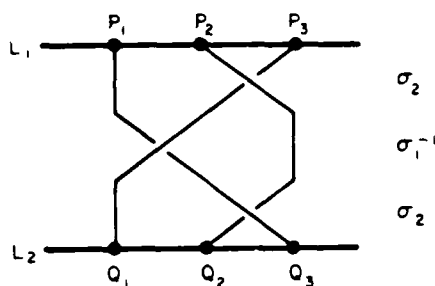


Fig. 6. Bus bars L_1 and L_2 connected by three strands of the braid defined by $\sigma_2\sigma_1^{-1}\sigma_2$.

Another type of chiral object is a braid of non-intersecting wires. Following Artin's theory of braids [14] we may describe a braid by projecting it on a plane and expressing the projected pattern as the product of terms, each of which is σ_i or σ_i^{-1} . Here σ_i denotes that the strand in position i crosses in front of the strand in position $i+1$ and σ_i^{-1} denotes that the latter crosses in front of the former.

Let us consider the three-stranded braid $\sigma_2\sigma_1^{-1}\sigma_2$ shown in Fig. 6. The bus bars L_1 and L_2 are connected by three flexible wires at the freely movable but ordered terminals P_1, P_2, P_3 and Q_1, Q_2, Q_3 . Clearly, the braid and bus bars form a chiral object. An incident wave will induce currents in the braid and bus bars and these currents will deform the configuration, viz., will make it more nearly planar, and thus reduce its chirality.

From these and other special cases we are led to the conjecture that the electrodynamic forces are such as to reduce or minimize chirality.

Conclusions

We direct attention to the interaction of electromagnetic fields with macroscopic chiral objects. By examining the wire helix and the wire braid as chiral objects, we obtain results which conform to the con-

jecture that composite media composed of macroscopic chiral objects are optically active, and to the conjecture that electrodynamic forces tend to reduce chirality. These considerations are expected to play a role in the development of diagnostic tools for remote sensing, in the design of electromagnetic shields and in the prediction of structural deformations.

Acknowledgement We thank Dr. J. P. Castillo for his interest in this work. This work was supported by the U.S. Air Force Office of Scientific Research under Grant No. AFOSR-77-3451.

References

1. F. M. Jaeger, *Lectures on the Principle of Symmetry* (Cambridge University Press, London 1917).
2. H. Weyl, *Symmetry* (Princeton University Press, Princeton 1952).
3. Louis Pasteur, *Ann. Chim. et Phys.* **24**, 442 (1848).
4. V. Prelog, *Chirality in Chemistry*, Nobel Lecture (Dec. 12, 1975), also in *Les Prix Nobel* (Imprimerie Royale P. A. Norstedt & Soner, Stockholm 1976).
5. C. W. Bunn, *Chemical Crystallography*, 2nd ed. (Oxford University Press, Oxford 1961).
6. J. F. Nye, *Physical Properties of Crystals* (Oxford University Press, Oxford 1957).
7. A. Sommerfeld, *Optics* (Academic Press, New York 1964).
8. See, e.g., S. L. Adler, R. F. Dashen, *Current Algebras* (W. A. Benjamin, New York 1968).
9. D. F. Arago, *Mém. Inst.* **1**, 93 (1811).
10. J. B. Biot, *Mém. Inst.* **1**, J (1812); *Mém. Acad. Sci.* **15**, 93 (1836).
11. K. F. Lindman, *Ann. Phys.* **63**, 621 (1920).
12. K. F. Lindman, *Ann. Phys.* **69**, 270 (1922).
13. W. H. Pickering, Experiment performed at Caltech (1945), private communication.
14. E. Artin, *Ann. Math.* **48**, 101 (1947); *Ann. Math.* **48**, 643 (1947).
15. See, e.g., W. Lietzmann, *Visual Topology* (American Elsevier Publishing Company, New York 1965).
16. S. A. Schelkunoff, H. T. Friis, *Antenna Theory and Practice* (John Wiley and Sons, New York 1952).
17. See, e.g., E. J. Post, *Formal Structure of Electromagnetics* (North-Holland, Amsterdam 1962).
18. G. Polya, G. Szegő, *Isoperimetric Inequalities in Mathematical Physics* (Princeton University Press, Princeton 1951), also *Am. J. Math.* **67**, 1 (1945).
19. See, e.g., D. Soper, *Classical Field Theory* (John Wiley & Sons, New York 1976) or J. E. Bjorken, S. D. Drell, *Relativistic Quantum Fields* (McGraw-Hill, New York 1965).

Steady State and Transient Electromagnetic Coupling Through Slabs

GIORGIO FRANCESCHETTI, SENIOR MEMBER, IEEE, AND CHARLES H. PAPAS, MEMBER, IEEE

Abstract—The problem of electromagnetic transmission through a slab where transmitting and receiving antennas are at finite distances from the slab is considered. The mathematical formulation of the problem is quite general. A detailed solution is presented for the case of a highly conducting slab exposed to sinusoidal and transient excitations. A discussion is given of the conditions under which measurements with the source and receiver at finite distances are equivalent to the same measurements with plane wave excitation.

I. INTRODUCTION

ONE OF THE simplest conceivable ways for determining the electromagnetic properties of materials is to measure the electromagnetic field transmitted through a slab of the material under test. The corresponding mathematical model consists of an infinite slab with transmitting and receiving antennas placed on opposite sides of the slab. The model provides a reasonably good approximation to the real situation of a slab of finite extent when the distance between transmitting and receiving points is small compared to the transverse slab dimensions.

Measurements can be made in the sinusoidal or the transient regime. For instance, MIL standards for evaluating the shielding effectiveness of materials [1] require that transmission measurements be made in the steady state at prescribed frequencies and then in a pulsed regime using wire and loop antennas placed at prescribed distances from the slab of shielding material. Although these standards are useful for relative comparisons, a fundamental question remains unanswered: does the measurement depend *only* on the electromagnetic properties of the slab (and on its thickness), or does it depend *also* on antenna type and orientation, antenna distance, and (for transient measurements) on transmitted waveform?

A crude but simple method for studying (or, at least, having an estimate of) the field coupled to the inside of an enclosure is to consider the transmission through a slab, provided the enclosure is large in terms of the incident wavelength. The slab may be perforated, inhomogeneous, or described by stochastic parameters, the last case being relevant to near-millimeter propagation through aerosols used for camouflage tactics. In electromagnetic pulse (EMP) experiments it is customary to simulate the EMP plane wave signal by using rather sophisticated antennas and guiding devices [2], [3]. An attractive alternative to this approach can result from an understanding and exploration of the role played by localized sources at finite distances from the test object.

The objectives of this paper are to reconsider the problem of steady-state and transient coupling through a slab with transmitting and receiving antennas located at finite distances from the slab, to cast the problem in an elegant form; and to show that, at least in the case of a highly conductive slab, simple analytical solutions to the problem can be obtained. An important result of the paper is the determination of antenna positions and (in the transient regime) of incident waveforms that will yield a transmitted field practically the same as that produced by plane wave excitation.

Transmission through highly conductive slabs is certainly not a new problem. For plane wave steady-state excitation, transmission line techniques can easily be applied [4]. For pulsed plane wave excitations, the solution is also available [5]. The situation is much less satisfactory for the case we want to study. It is not the aim of this paper to provide a full bibliography on this subject (for a more complete bibliography see [6]). We note only that the first attempt to solve this problem was made in 1936 [7] by accommodating the classical results of Maxwell on eddy currents and thin shields to the case of two coaxial loops separated by a plane conducting sheet. Early studies on antenna coupling through plane shields were based on low-frequency [8], [9] or quasi-static [10] approximations, were mainly relative to loop excitation [8]–[10], and required numerical computation [8]–[12] of integral expressions for the transmitted field. Although the validity of the simple transmission line theory [4] for antennas at finite distances from the shield, or shields of finite extent, has been questioned [13], it appears that all expressions derived in the referenced literature resemble Schelkunoff's formulas [14].

Due to the symmetry of the problem it can easily be surmised that plane wave expansion techniques provide a powerful tool of analysis for an arbitrary type of excitation of an infinite slab. These techniques have been recently applied [14], [15] to the case of electric or magnetic dipole excitation in parallel (dipoles parallel to the slab) or coaxial (dipoles normal to the slab) configuration, by computing the transmitted field through the use of fast Fourier numerical programs. In this paper we shall use the same approach. However, we will show that, although the Fourier transformation of the fields is a logical intermediate step of the analysis, it is not needed in the final formulation of the solution. Indeed, the solution can be conveniently expressed in terms of a convolution integral, wherein the presence of the slab is described by an appropriate transfer function. Then, at least for antennas in coaxial configuration, the convolution integral can be analytically evaluated both in steady-state and transient regimes, and no numerical work is necessary. Inspection of the solution allows us to answer the original question about the influence of the finite antenna separation on measurements. After all the mathematical machinery has been worked out and simple, physically sound, understandable results are obtained, a discussion of the final results is presented in Section VI.

Manuscript received November 7, 1978; revised March 30, 1979. This work was supported by the U.S. Air Force Office of Scientific Research under Grant No. AFOSR-77-3451.

G. Franceschetti is with the Electrical Engineering Department, California Institute of Technology, Pasadena, CA 91125, on leave from the University of Naples, Italy.

C. H. Papas is with the Electrical Engineering Department, California Institute of Technology, Pasadena, CA 91125.

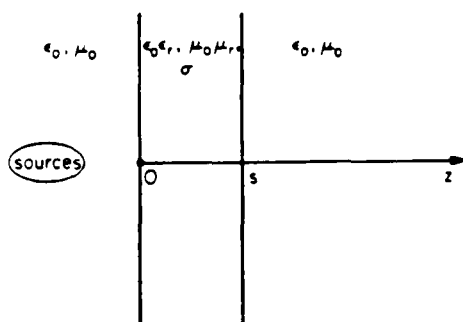


Fig. 1. Geometry of problem.

II. CIRCUIT-LIKE ANALYSIS OF ELECTROMAGNETIC TRANSMISSION THROUGH A SLAB

With reference to Fig. 1, let us consider an infinite slab of thickness s and characterized, in the frequency domain, by permittivity $\epsilon = \epsilon_0 \epsilon_r$, permeability $\mu = \mu_0 \mu_r$, and conductivity σ . We want to compute the field $\mathbf{E}^t, \mathbf{H}^t$ transmitted at $z > s$ along the z axis when the incident field $\mathbf{E}^i, \mathbf{H}^i$, i.e., the field produced by the sources when the slab is removed, is known at $z = 0$. For this purpose it is convenient to expand the incident field in a plane wave set, since the interaction of individual plane wave components with the slab can be conveniently taken into account.

Accordingly, let $H_z^i(x, y, 0), E_z^i(x, y, 0)$ be the z components of the field incident on the slab surface, with an assumed time dependence $\exp(j\omega t)$. The corresponding spectral components $h_z^i(u, v), e_z^i(u, v)$ are given, at $z = 0$, by

$$h_z^i(u, v) = \frac{1}{(2\pi)^2} \int_{-\infty}^{+\infty} dx \int_{-\infty}^{+\infty} dy H_z^i(x, y, 0) \cdot \exp(jux + jvy) \quad (2.1)$$

$$e_z^i(u, v) = \frac{1}{(2\pi)^2} \int_{-\infty}^{+\infty} dx \int_{-\infty}^{+\infty} dy E_z^i(x, y, 0) \cdot \exp(jux + jvy) \quad (2.2)$$

At $z = s$, i.e., at the output of the slab, the spectral components $h_z^t(u, v), e_z^t(u, v)$ will be linearly related to the incident components (2.1) and (2.2) in the case of a slab made of a linear material. Hence,

$$h_z^t(u, v) = t_H(u, v) h_z^i(u, v) \quad (2.3)$$

$$e_z^t(u, v) = t_E(u, v) e_z^i(u, v) \quad (2.4)$$

The transfer coefficients t_H, t_E can be easily computed for a homogeneous isotropic slab by noting that the transverse spectral components $h_t(u, v), e_t(u, v)$ are related to the longitudinal ones $h_z(u, v), e_z(u, v)$ via the following relations:

$$h_t = \frac{\omega \epsilon e_z \kappa x^2 + w h_z^2 \kappa x^2}{u^2 + v^2} \quad (2.5)$$

$$e_t = \frac{-\omega \mu h_z \kappa x^2 + w e_z^2 \kappa x^2}{u^2 + v^2} \quad (2.6)$$

wherein $\kappa = u^2 + v^2 + w^2$ and is the propagation vector referring to a Cartesian system of unit vectors $\hat{x}, \hat{y}, \hat{z}$, and the upper (lower) signs refer to waves propagating in the positive (negative) direction of the z axis. Equations (2.5) and (2.6) represent the total spectral field as a superposition of TE ($e_z = 0$) and TM ($h_z = 0$) parts. With the medium being identical at both sides of the slab, it is then evident that t_H coincides with the usual slab transmission coefficient for TE plane wave incidence and, similarly, t_E is the same as the slab transmission coefficient for TM plane wave incidence. Letting

$$w = \sqrt{\kappa^2 - (u^2 + v^2)},$$

$$w_s = \sqrt{\kappa^2 \left(\epsilon_r + \frac{\sigma}{j\omega \epsilon_0} \right) \mu_r - (u^2 + v^2)}, \quad (2.7)$$

$$\gamma_H = \frac{w_s}{\mu_r w}, \quad \gamma_E = \frac{j\omega \epsilon_0}{\sigma + j\omega \epsilon_0 \epsilon_r} \frac{w_s}{w} \quad (2.8)$$

we have

$$t(u, v) = \frac{4}{(1 + \gamma)^2} \frac{\exp(-jw_s s)}{1 - \left(\frac{1 - \gamma}{1 + \gamma} \right)^2 \exp(-2jw_s s)} \quad (2.9)$$

wherein γ may be taken equal to γ_H or γ_E in order to obtain t_H or t_E , respectively, and $\kappa = \omega \sqrt{\epsilon_0 \mu_0}$.

The spectral components h_z, e_z at any $z > s$ are equal to the corresponding values (2.3) and (2.4) at $z = s$ times the plane wave transfer function $\exp[-jw(z - s)]$. Accordingly, the z component $F_z^t(x, y, z)$ of the field transmitted at any arbitrary abscissa $z > s$ will be expressed in terms of the double Fourier integral

$$F_z^t(x, y, z) = \int_{-\infty}^{+\infty} du \int_{-\infty}^{+\infty} dv f_z^t(u, v) t(u, v) \cdot \exp[-jw(z - s)] \cdot \exp(-jux - jvy) \quad (2.10)$$

wherein f_z^t may be taken equal to h_z^t or e_z^t and, correspondingly, the values of t_H or t_E should be used.

On the other hand, the spectral representation of the z components of the incident field (the slab is now removed) at any abscissa z is obviously the following:

$$F_z^i(x, y, z) = \int_{-\infty}^{+\infty} du \int_{-\infty}^{+\infty} dv f_z^i(u, v) \exp(-jwz) \cdot \exp(-jux - jvy) \quad (2.11)$$

Comparison of (2.10) and (2.11) shows that the transmitted field can be computed as the double convolution of the incident field and the double Fourier transform of $t(u, v) \exp(jws)$, hence

$$F_z^t(x, y, z) = \frac{1}{(2\pi)^2} \int_{-\infty}^{+\infty} dx' \int_{-\infty}^{+\infty} dy' F_z^i(x', y', z) \cdot T(x - x', y - y') \quad (2.12)$$

$$T(x, y) = \int_{-\infty}^{+\infty} du \int_{-\infty}^{+\infty} dv t(u, v) \exp(j\omega s) \cdot \exp(-jux - jvy) \quad (2.13)$$

In the words of system theory F^t is identified with the output of a linear system described by the unit response function (2.13) and excited by the input F^i .

We further note that relations similar to (2.12) exist between the transmitted and incident transverse components of the field, as easily follows from (2.5) and (2.6). It is only necessary to decompose the incident field in its TE and TM parts and then to apply superposition.

III. THE AZIMUTHALLY SYMMETRIC CASE

A case of particular interest is obtained when the incident field does not depend on x and y separately but rather upon the transverse coordinate $\rho = \sqrt{x^2 + y^2}$. For instance, if the source is taken equal to an elementary electric or magnetic dipole parallel to the z axis at $P(0, 0, -d)$, then

$$F_z^i(x, y, z) = F_z^i(\rho, z) = -\frac{j\omega}{\kappa^2} [\kappa^2 \mathbf{A} + \nabla \nabla \cdot \mathbf{A}] \cdot \hat{z} \\ = -\frac{j\omega}{\kappa^2} \left[\kappa^2 A + \frac{\partial^2 A}{\partial z^2} \right] = \frac{j\omega}{\kappa^2} \frac{1}{\rho} \frac{\partial}{\partial \rho} \rho \frac{\partial A}{\partial \rho} \quad (3.1)$$

wherein

$$A(\rho, z) = C \frac{\exp(-j\kappa\sqrt{\rho^2 + (d+z)^2})}{\sqrt{\rho^2 + (d+z)^2}} \quad (3.2)$$

is an electric or magnetic vector potential, the source intensity being proportional to the constant C .

The integrals (2.12) and (2.13) can now be simplified by using the change of coordinates:

$$x = \rho \cos \phi, \quad y = \rho \sin \phi, \quad u = \xi \cos \psi, \quad v = \xi \sin \psi. \quad (3.3)$$

Accordingly,

$$T(x, y) = T(\rho) = \int_0^\infty \xi d\xi t(\xi) \exp(j\sqrt{\kappa^2 - \xi^2} s) \\ \cdot \int_0^{2\pi} \exp[-j\rho\xi \cos(\psi - \phi)] d\psi \\ = 2\pi \int_0^\infty \xi d\xi J_0(\rho\xi) t(\xi) \exp(j\sqrt{\kappa^2 - \xi^2} s), \quad (3.4)$$

and the field transmitted on the axis is given by

$$F_z^t(0, 0, z) = \int_0^\infty \rho d\rho F_z^i(\rho, d+z) T(\rho) \\ = \int_0^\infty \xi d\xi \exp(j\sqrt{\kappa^2 - \xi^2} s) t(\xi) \\ \cdot \int_0^\infty \rho d\rho F_z^i(\rho, d+z) J_0(\xi\rho) \quad (3.5)$$

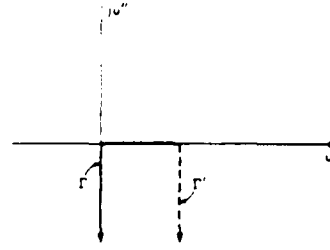


Fig. 2. Integration path in complex u plane.

wherein the order of integration has been reversed. Upon substitution of (3.1) in (3.5) the inner integral can be evaluated by repeated integration by parts as follows:

$$\int_0^\infty \rho d\rho F_z^i(\rho, d+z) J_0(\rho\xi) \\ = -\frac{j\omega C}{\kappa^2} \xi^2 \int_0^\infty \frac{\rho \exp(-j\kappa\sqrt{\rho^2 + (d+z)^2})}{\sqrt{\rho^2 + (d+z)^2}} J_0(\rho\xi) d\rho \\ = -\frac{\omega C}{\kappa^2} \xi^2 \frac{\exp[-j\sqrt{\kappa^2 - \xi^2}(d+z)]}{\sqrt{\kappa^2 - \xi^2}} \quad (3.6)$$

the last expression stemming from a known Fourier-Bessel transform [16]. Note that $\sqrt{\kappa^2 - \xi^2} = -j\sqrt{\xi^2 - \kappa^2}$ for $\xi^2 > \kappa^2$ and that we have implicitly assumed $\kappa \neq 0$ in this section.

The formal expression for the z component of the field transmitted through the slab is now the following:

$$F_z^t(0, 0, z) = \omega C \kappa \int_\Gamma (1-u^2) t(u) \exp(-j\kappa l u) du \quad (3.7)$$

wherein $l = d - s + z$, the integration path Γ is depicted in Fig. 2, and the substitution $\kappa^2 - \xi^2 = \kappa^2 u^2$ has been used.

IV. THE CASE OF AN ELECTRIC PLANE SHIELD-STEADY-STATE EXCITATION

A case particularly interesting for applications is obtained when $\mu_r = 1$, $\sigma \gg \omega\epsilon_0\epsilon_r$, i.e., when a highly conducting non-magnetic slab is used as a shielding screen. As already noted in Section I, this is an important configuration in shielding theory and practice. The solution to this problem is available in numerical form [14], [15] for prescribed sinusoidal time variation and arbitrary spatial dependence for the fields, and in analytical form [5] for prescribed plane wave excitation and arbitrary time variation.

The case of a magnetic dipole excitation is considered first. The expression for $t(u)$ pertinent to this case is the following:

$$t_H(u) = \frac{4u\sqrt{\alpha^2 + u^2}}{(u + \sqrt{\alpha^2 + u^2})^2} \\ \cdot \frac{\exp(-j\sqrt{\alpha^2 + u^2} \kappa s)}{1 - \left[\frac{u - \sqrt{\alpha^2 + u^2}}{u + \sqrt{\alpha^2 + u^2}} \right]^2 \exp(-2j\sqrt{\alpha^2 + u^2} \kappa s)} \quad (4.1)$$

$$\alpha^2 = \frac{\sigma + j\omega\epsilon_0(\epsilon_r - 1)}{j\omega\epsilon_0} \cong \frac{\sigma}{j\omega\epsilon_0} \quad (4.2)$$

It is noted that $t_H(u)$ exhibits no singularity in the lower right quadrant of the complex u plane, so that the integration path Γ can be freely deformed therein, e.g., in the new path Γ' (see Fig. 2). When (4.1) is substituted in (3.7) it is noted that we can neglect u^2 with respect to α^2 provided the integrand is negligible when $u > |\alpha|$. Accordingly, when $\kappa l / |\alpha| \gg 1$ the integral (3.7), specified to the case at hand, becomes

$$H_z^t(0, 0, l) = -j\omega C\kappa \frac{4}{\alpha} \frac{\exp(-j\alpha\kappa s)}{1 - \exp(-2j\alpha\kappa s)} \exp(-j\kappa l) \cdot \int_0^\infty u(-jv^2 + 3v + 2j) \exp(-\kappa lv) dv, \quad (4.3)$$

and the origin of coordinates is now in correspondence to the source. The integral is now straightforward to evaluate and can be conveniently normalized to the value of the incident field $H_z^i(0, 0, l)$. We have

$$\frac{H_z^t(0, 0, l)}{H_z^i(0, 0, l)} = \left[\frac{4}{\alpha} \frac{\exp(-j\alpha\kappa s)}{1 - \exp(-2j\alpha\kappa s)} \right] \left[\frac{1 + \frac{3}{j\kappa l} + \frac{3}{(j\kappa l)^2}}{1 + \frac{1}{j\kappa l}} \right] = t_0(\alpha, \kappa s) \Omega_H(\kappa l). \quad (4.4)$$

It is noted that the first bracketed term $t_0(\alpha, \kappa s)$ is just the plane wave transmission coefficient under normal incidence and appropriate to a highly conducting screen. The second term $\Omega_H(\kappa l)$ depends on the mutual distance l between transmitting and receiving points and approaches 1 when $\kappa l \gg 1$. Accordingly, it follows that a simple plane wave transmission coefficient can be used for evaluating shielding effectiveness provided that transmitting and receiving antennas are a few wavelengths apart.

On the other hand, when κl is small, $\Omega_H(\kappa l) \cong 3/j\kappa l$, and

$$\frac{H_z^t(0, 0, l)}{H_z^i(0, 0, l)} \cong \frac{3}{j\kappa l} t_0(\alpha, \kappa s) = \frac{\exp(-j\alpha\kappa s - j\pi/4) 3\delta}{[1 - \exp(-2j\alpha\kappa s)] \sqrt{2} l}, \quad (4.5)$$

wherein δ is the skin depth of the screen. Note that (4.5) is valid provided that $\delta/l \ll 1$; otherwise the assumption $\kappa l \gg 1$ is no longer met.

The case of an electric dipole excitation can be treated similarly. We have

$$E_z^t(u) = \frac{4\alpha^2 u \sqrt{\alpha^2 + u^2}}{(\alpha^2 u + u + \sqrt{\alpha^2 + u^2})^2} \cdot \frac{\exp(-j\sqrt{\alpha^2 + u^2} \kappa s)}{1 - \left(\frac{\alpha^2 u + u - \sqrt{\alpha^2 + u^2}}{\alpha^2 u + u + \sqrt{\alpha^2 + u^2}} \right)^2 \exp(-2j\sqrt{\alpha^2 + u^2} \kappa s)} \quad (4.6)$$

We can now neglect u^2 with respect to α^2 without serious limitation in the validity of the results. The integral corresponding

to (4.3) is the following:

$$E_z^t(0, 0, l) = \omega C\kappa t_0(\alpha, \kappa s) \cdot \left\{ \int_1^\infty \frac{\exp(-j\kappa l u)}{u} du + j \int_0^\infty (1 - ju) \exp(-\kappa l v) dv \right\} \quad (4.7)$$

which can be easily evaluated to yield

$$\frac{E_z^t(0, 0, l)}{E_z^i(0, 0, l)} = t_0(\alpha, \kappa s) \Omega_E(\kappa l) \quad \Omega_E(\kappa l) = \frac{1}{2} \frac{1 + j\kappa l + (j\kappa l)^2 \exp(j\kappa l) [Ci(\kappa l) - jSi(\kappa l)]}{1 + \frac{1}{j\kappa l}} \quad (4.8)$$

wherein the cosinus integral $Ci(x)$ and sinus integral $Si(x)$ functions [17] do appear.

It is again noted that $\Omega_E(\kappa l) \rightarrow 1$ when $\kappa l \gg 1$, as easily follows upon use of the asymptotic series expansions [17] of the functions $Ci(x)$ and $Si(x)$, so that (4.8) reduces again to the plane wave transmission coefficient $t_0(\alpha, \kappa s)$ provided that transmitting and receiving antennas are a few wavelengths apart. On the contrary, when κl is small, a proper series expansion [17] shows that $\Omega_E(\kappa l) \cong j\kappa l/2$ and

$$\frac{E_z^t(0, 0, l)}{E_z^i(0, 0, l)} \cong \frac{j\kappa l}{2} t_0(\alpha, \kappa s) = j \frac{\exp(-j\alpha\kappa s + j\pi/4)}{1 - \exp(-2j\alpha\kappa s)} (\kappa l)^2 \frac{\delta}{\sqrt{2} l}. \quad (4.9)$$

V THE CASE OF AN ELECTRIC PLANE SHIELD—TRANSIENT EXCITATION.

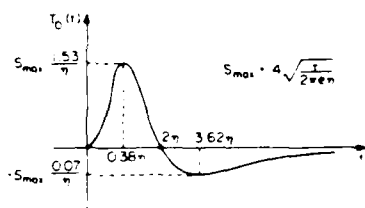
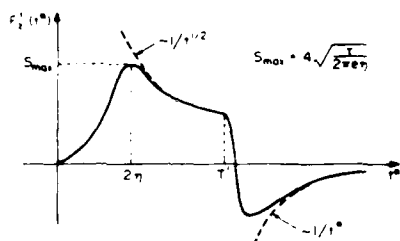
We have shown in Section IV that the steady-state z components of the field transmitted through a highly conducting plane shield are given by

$$F_z^t(0, 0, l) = F_z^i(0, 0, l) t_0(\alpha, \kappa s) \Omega(\kappa l). \quad (5.1)$$

It is then evident that the z component of the transient transmitted field can be obtained by time-convolving the transient z components of the incident field with the inverse Fourier transforms of $t_0(\omega)$ and $\Omega(\omega)$, let us say $T_0(t)$ and $\Omega(t)$. Use of Laplace inversion tables [18] shows that

$$\begin{aligned} T_0(t) &= 2 \sqrt{\frac{\tau}{\pi}} \sum_{n=1}^{\infty} \frac{\exp(-n^2 \eta / \tau)}{t^{3/2}} (2n^2 \eta - t) \\ &= 4 \sqrt{\frac{\tau}{\pi}} \sum_{n=1}^{\infty} \frac{d}{dt} \frac{\exp(-n^2 \eta / \tau)}{t^{1/2}} \\ &= 4 \sqrt{\frac{\tau}{\pi}} \sum_{n=1}^{\infty} \frac{d}{dt} S_0(t) \end{aligned} \quad (5.2)$$

where $\tau = \epsilon_0 / \sigma$ and is the relaxation time of the material of the shield, and $\eta = s^2 / (c^2 \tau)$ and is the diffusion time through the shield thickness.

Fig. 3 Qualitative behavior of first series term of function $T_0(t)$ Fig. 4 Qualitative behavior of pulsed field of time duration T after transmission through a highly conductive slab

A qualitative behavior of the first term $n = 1$ of $T_0(t)$ is given in Fig. 3, wherein $S_{\max} = 4\sqrt{\eta/2\pi\epsilon\eta} = S_0(2\eta)$ and is the maximum value of the function $S_0(t)$ (see also Fig. 4), where in S_{\max} "e" is the Neper's constant

The behavior of successive terms of the series (5.2) is similar to that depicted in Fig. 3. The maxima occur at later times and their absolute values are smaller by the factor $\exp[-2.6(n^2 - 1)]/n^3$. Accordingly, they can be safely neglected, and we can take only the first term of the series (5.2).

After some algebra Laplace inversion [19] of the two functions $\Omega(\omega)$ leads to

$$\Omega_H(t) = \delta(t) + \frac{3 - \exp(-t/T)}{T} U(t) \quad (5.3)$$

$$\Omega_E(t) = \delta(t) - \frac{2}{T} \exp(-t/T) U(t) + \frac{3}{T} \int_0^T \frac{\exp(-u)}{\left(1 + \frac{t}{T} - u\right)^4} du \quad (5.4)$$

where $\delta(t)$ and $U(t)$ are the Dirac and the unit step function, respectively, $T = l/c$ and is the free-space transit time from the transmitting to the receiving antenna.

Convolution of (5.2) with the $\delta(t)$ terms of (5.3) and (5.4) just reproduce the function $T_0(t)$. Convolution with the other terms may become significant only after a time of order T . Accordingly, if the incident field has a time duration small compared with T , i.e., its spatial length is small compared with the in-between antennas distance l , then the time dependence of the transmitted field is simply given by the time convolution of the incident signal and the function $T_0(t)$. This transmitted field is the same as would be obtained for the case of plane wave excitation. Accordingly, the result is obtained that the finite distance between antennas plays no significant role if the incident waveform is sufficiently short in time. For in-

stance, if the incident signal is a pulse of unit amplitude and time duration T' , then

$$F_z^+(0, 0, l, t^*) = 4 \sqrt{\frac{\tau}{\pi}} \frac{\exp\left(-\frac{\eta}{t^*}\right)}{\sqrt{t^*}}, \quad t^* \leq T' \quad (5.5)$$

$$F_z^+(0, 0, l, t^*) = 4 \sqrt{\frac{\tau}{\pi}} \left\{ \frac{\exp\left(-\frac{\eta}{t^*}\right)}{\sqrt{t^*}} - \frac{\exp\left(-\frac{\eta}{t^* - T'}\right)}{\sqrt{t^* - T'}} \right\}, \quad t^* > T' \quad (5.6)$$

where $t^* = t - (l/c)$ and is the retarded time. A qualitative sketch of (5.5) and (5.6) is given in Fig. 4 for $T' > 2\eta$. When $T' \ll 2\eta$, then the transmitted field is just given by (5.2) times T' .

VI CONCLUSIONS AND PRACTICAL CONSIDERATIONS

We have considered the problem of the transmission of steady-state and transient electromagnetic waves through a slab. An analytical solution has been obtained for the case of a linear homogeneous isotropic highly conducting infinite slab excited by collinear electric or magnetic dipoles. The transmitted z components of the field are expressed as the product (steady-state case) or the convolution (transient case) of the corresponding incident field components and a two-term factor. In the frequency domain the first term of this factor (see (5.1)) is exactly the transmission coefficient of a plane wave normally incident on the slab. The second term takes into account the finite distance between the transmitting and receiving antennas and becomes significant only when this distance is of the order of, or smaller than, the free-space wavelength (steady-state case) or the spatial length of the incident pulse (transient case). It is therefore possible to obtain plane wave excitation results even when sources (and receivers) are located at finite distances. For this all that is needed is the proper choice of distance between antennas.

It is certainly true that these results have been obtained under the conditions that the transmitting antenna is a dipole oriented normal to the slab, that the transmitted field is computed along the axial direction of the dipole, and that only the z components of the field are used in the comparison. However, we believe that our analysis has a more general validity. For instance, results of the collinear configuration can easily be extended to transmitted field points off the axis. We should only substitute

$$J_0(\xi\sqrt{\rho^2 + \rho'^2 - 2\rho\rho'\cos\phi'}) \quad (6.1)$$

for $J_0(\xi\rho)$ in (2.12). Then expansion [20] of the Bessel function (6.1) and integration in ϕ' gives

$$F_z^+(\rho, l) = \omega C k \int_0^1 (1 - u^2) t(u) J_0(k\rho\sqrt{1 - u^2}) \cdot \exp(-k|u|) du \quad (6.2)$$

which is the generalization of (3.7) to the case $\rho \neq 0$. Then $\partial F_z(\rho, l)/\partial \rho = 0$ for $\rho = 0$, which implies that the results of our analysis are certainly also valid in the neighborhood of the axis. Furthermore, use of Maxwell's equations, with (6.2) as the longitudinal field, shows that the same is true for transverse fields. In this extension, however, the simplifying assumptions used in the body of this paper should be checked again. Should further study show that the above considerations can be extended to more complicated geometries, all simulation studies for shielding purposes might be worth reconsidering.

Some few practical notes are now in order. Reference is made to a copper slab ($\sigma = 5.8 \times 10^7$ S/m) of thickness $s = 1$ mm, so that $\tau = 1.52 \times 10^{-19}$ s and $\eta = 70$ μ s. Only the plane wave transmission coefficient will be considered. For incident pulses of unit amplitude and time duration $T' \ll \eta$, the peak of the transmitted field is equal to $2.7 \times 10^{-7} T'/\eta$, therefore linearly decreasing with the bandwidth ($\sim 1/T'$) of the signal. In the sinusoidal excitation case the attenuation due to the mismatch $4|\alpha|$ equals that due to the damping inside the slab material $\exp(-|\alpha|ks/\sqrt{2})$ at the frequency $f = 0.72$ MHz. At this frequency the transmitted field is equal to 11×10^{-12} times the incident one. At higher frequencies the signal is decreasing exponentially with the square root of the frequency.

For moderate antenna spacings it is noted that the transmitted field can be computed using the plane wave transmission coefficient only when the attenuation is very high. However, this may not be the case if even small apertures exist in the screen. Accordingly, we believe it is worthwhile to extend the analysis presented in this paper to other canonical problems, which are amenable to the same analytical approach. Among those, we list the problem of an infinite conductive screen with a single hole and that of a conductive screen with a regular lattice of equal small apertures. The former problem can take advantage of the solution of a plane wave diffraction by apertures in conducting screens [21]–[23] and, eventually, of symmetrization procedures [24]. The latter could make use of the artificial dielectric theory [25] properly accommodated to this single sheet problem.

REFERENCES

- [1] Anonymous, "Methods of attenuation measurements for enclosures, electromagnetic shielding, for (SIC) electronic test purposes," Dept. Defense, MIL-Standard STD-285, June 25, 1956.
- [2] C. E. Baum, E. L. Breen, J. C. Giles, J. O'Neill, and G. D. Sower, "Sensors for electromagnetic pulse measurements both inside and away from nuclear source regions," *IEEE Trans. Antennas Propagat.*, vol. AP-26, no. 1, pp. 22–35, Jan. 1978.
- [3] C. E. Baum, "EMP Simulators for various types of nuclear EMP environment: An interim categorization," *IEEE Trans. Antennas Propagat.*, vol. AP-26, no. 1, pp. 35–53, Jan. 1978.
- [4] S. A. Schelkunoff, *Electromagnetic Waves*. Princeton, NJ: Van Nostrand, 1943, pp. 223–225 and 303–306.
- [5] W. J. Karzas and T. C. Mo, "Linear and nonlinear EMP diffusion through a ferromagnetic conducting slab," *IEEE Trans. Antennas Propagat.*, vol. AP-26, no. 1, pp. 118–129, Jan. 1978 (see also, T. C. Mo, RDA Rep. TR-9000-001, July 1975, sect. 2.2 and appendix C; and T. C. Mo, AFWL Rep. EMP-3-291.)
- [6] G. Franceschetti, "Fundamentals of steady-state and transient electromagnetic field in a shielding enclosure," Communications Lab., Univ. Illinois at Chicago Circle, Rep. 77-2, 1977.
- [7] S. Levy, "Electromagnetic shielding effect of an infinite plane conducting sheet placed between circular coaxial loops," *Proc. IRE*, vol. 21, no. 6, pp. 923–941, 1936.
- [8] J. R. Moser, "Low-frequency shielding of a circular loop electromagnetic field source," *IEEE Trans. Electromagn. Compat.*, vol. EMC-9, no. 1, pp. 6–18, 1967.
- [9] R. R. Bannister, "New theoretical expressions for predicting shielding effectiveness for the plane shield case," *IEEE Trans. Electromagn. Compat.*, vol. EMC-10, no. 1, pp. 2–7, 1968.
- [10] —, "Further notes for predicting shielding effectiveness of the plane shield case," *IEEE Trans. Electromagn. Compat.*, vol. EMC-11, no. 2, pp. 50–53, 1969.
- [11] C. M. Ryan, "Computer expressions for predicting shielding effectiveness for the low-frequency plane shield case," *IEEE Trans. Electromagn. Compat.*, vol. EMC-10, no. 2, pp. 83–94, 1967.
- [12] L. F. Babcock, "Computer determination of electromagnetic wave shielding effectiveness," *IEEE Trans. Electromagn. Compat.*, vol. EMC-10, no. 6, pp. 331–334, 1968.
- [13] J. E. Bridges and D. A. Miller, "Comparison of shielding calculations," *IEEE Trans. Electromagn. Compat.*, vol. EMC-10, no. 1, pp. 175–176, 1968 (see also, in the same issue, R. B. Shultz, Editor's reply, pp. 176–177).
- [14] E. Villaseca, W. Blackwood, and C. Davis, "Application of plane wave spectrum to EMP shielding effectiveness," Ann. Conf. Nuclear and Space Radiation Effects, College of William and Mary, Williamsburg, VA, July 12–15, 1977.
- [15] E. Villaseca and L. Bowers, "Application of the plane wave spectrum to EMP shielding effectiveness," URSI Symp., Univ. of Maryland, May 15–19, Washington, D. C., 1978.
- [16] W. Magnus, F. Oberhettinger, and F. G. Tricomi, *Tables of Integral Transforms*, vol. 2, A. Erdélyi, Ed. New York: McGraw-Hill, 1954, p. 9, (25).
- [17] —, *Higher Transcendental Functions*, vol. 2, A. Erdélyi, Ed. New York: McGraw-Hill, 1953, p. 145, eqs. (1), (2); p. 146, eqs. (8), (9).
- [18] G. E. Roberts and H. Kaufman, *Table of Laplace Transforms*. Philadelphia and London: Saunders Co., 1966, p. 246, eq. (15).
- [19] W. Magnus, F. Oberhettinger, and F. G. Tricomi, *Tables of Integral Transforms*, vol. 1, A. Erdélyi, Ed. New York: McGraw-Hill, 1954, p. 268, eq. (31).
- [20] I. S. Gradshteyn and I. M. Ryzhik, *Table of Integrals, Series and Products*. New York: Academic, 1965, p. 979, eq. (WA391).
- [21] H. A. Bethe, "Theory of diffraction by small holes," *Phys. Rev.*, vol. 60, pp. 163–182, 1942.
- [22] J. Meixner and W. Andrejewski, "Strenge Theorie der Beugung ebener elektromagnetischer Wellen der vollkommen leitenden ebenen Schirme," *Ann. Phys.*, vol. 7, pp. 157–168, 1950.
- [23] W. Andrejewski, "Die Beugung elektromagnetischer Wellen an der leitenden Kreisscheibe und der kreisförmigen Öffnung in leitenden ebenen Schirmen," *Z. Angew. Phys.*, vol. 5, pp. 178–186, 1953.
- [24] D. L. Jaggard and C. H. Papas, "On the application of symmetrization to the transmission of electromagnetic waves through small convex apertures of arbitrary shape," *Appl. Phys.*, vol. 15, pp. 21–25, 1978.
- [25] R. E. Collin, *Field Theory of Guided Waves*. New York: McGraw-Hill, 1960, ch. 12, pp. 509–551.
- [26] W. C. Kuo and K. K. Mei, "Numerical approximation of the Sommerfeld integral for fast convergence," *Radio Sci.*, vol. 13, pp. 407–415, 1978.
- [27] D. C. Chang and R. J. Fisher, "A unified theory of radiation of a vertical electric dipole above a dissipative earth," *Radio Sci.*, vol. 9, pp. 1129–1138, 1974.
- [28] J. R. Wait, "Induction in a conductive sheet by a small current-carrying loop," *Appl. Sci. Res.*, vol. B-3, pp. 230–235, 1953.
- [29] J. R. Wait, "The electromagnetic fields of a dipole in the presence of a thin plasma sheet," *Appl. Sci. Res.*, vol. B-8, pp. 397–417, 1961.



Giorgio Franceschetti (S'60-M'62-SM'73) was born in Naples, Italy, in March, 1935. He graduated with degrees in electrical engineering from the University of Naples, Italy, and from the Higher Institute for Telecommunication, Rome, Italy, in 1959 and 1961, respectively. In 1965 he obtained the Libera Docenza from the Ministry of Education, Rome, Italy.

Winner of a national competition, he was appointed Full Professor of Electromagnetic Waves at the University of Naples, Italy, and

has been there since 1968. He was a Visiting Professor at the University of Illinois, Chicago Circle, from 1976 to 1977 and during the winter of 1979. During the summer of 1978 he was a Research Associate at the California Institute of Technology, Pasadena. He is also Associate Editor of *Alta Frequenza*.

Mr. Franceschetti was a Fulbright Scholar at the California Institute of Technology, Pasadena.

Charles H. Papas (S'41-A'42-M'55) was born in Troy, NY, on March 29, 1918. He received the B.S. degree in electrical engineering from the Massachusetts Institute of Technology, Cambridge, in 1941. He received the M.S. degree in communication engineering and the Ph.D. degree in electrodynamics from Harvard University, Cambridge, MA, in 1946 and 1948, respectively.



From 1941 to 1945 he was with the U.S. Navy, working first on the degaussing problem at the Naval Ordnance Laboratory and then on the design of radio and radar antennas at the Bureau of Ships. From 1948 to 1950 he was a Research Fellow at Harvard, working with Prof. R. W. P. King on electromagnetic boundary-value problems and antenna theory. From 1950 to 1952 he was with the University of California as Assistant Professor in Berkeley and Staff Member in Los Alamos. In 1952, to work with Prof. W. R. Smythe, he moved to the California Institute of Technology where he is currently Professor of Electrical Engineering. His research interests have centered on electromagnetic theory and its applications to antennas, propagation, gravitational electrodynamics, and astrophysics.

Dr. Papas was elected a foreign member of the Academy of Sciences, Yerevan, USSR, for his work in radiophysics.

Mechanical Forces and Torques Associated with Electromagnetic Waves

G. Franceschetti* and C. H. Papas

California Institute of Technology, Pasadena, CA 91125, USA

Received 4 March 1980/Accepted 19 June 1980

Abstract. Mechanical forces and torques associated with electromagnetic waves impinging on several objects are computed. The incoming radiation can be linearly or circularly polarized, thus carrying linear and angular momenta. The objects are matched dipoles in several configurations and a metal sphere. Numerous interesting results are obtained.

PACS: 02. 41

It is well known that an electromagnetic wave exerts forces and (possibly) torques on charges and currents and that the mathematical description of these mechanical actions is given by the Lorentz force equation, which connects electromagnetic and mechanical phenomena. If an electromagnetic wave interacts with, say, a metal body, charges and currents are induced, and hence the body becomes subject to local forces and torques. When a spatial summation is made, the total time-dependent (body) force and (body) torque acting on the object are obtained.

It is usually believed that these forces and torques are "small" and hence negligible from the viewpoint of engineering application. However, this is not always so. As a matter of fact, a strong interest in this area is now emerging. For instance, a book recently has appeared [1] which gives a most complete review of existing theoretical and experimental methods for determining electromagnetic signals by means of their associated mechanical effects. Electromagnetic pulses (EMP) produced by nuclear explosion in the upper atmosphere is another case of recent interest. Also satellite applications have attracted considerable attention, where the (relatively) small mass of the object and the cumulative nature of the mechanical actions (translation or rotation) can produce long-range macroscopic effects. Mechanical effects can be used, for example, to steer the satellite by radiating suitably polarized electromagnetic fields from the satellite. And even key operations, as deploying antennas, can be

performed, in principle, by injecting transient currents into the structures. There are cases in which the movement of a metal object in an electromagnetic field can produce additional mechanical stresses. For instance, the propellers of a helicopter, which may be roughly modeled as rotating dipoles, can be further stressed when exposed to an incident electromagnetic field.

Accordingly, we believe that it is useful to examine a number of very simple cases of interaction between metal objects and electromagnetic fields, and to compute the resulting mechanical forces and torques. As the metal object, we have considered the simplest one – the tuned electric dipole – in several configurations: stationary, translational, rotational, receiving, transmitting, where the electric dipole is isolated or coupled with a magnetic dipole as a turnstile antenna or a chiral antenna. We have computed the body force and torque acting on the dipole and its time average, for the case of an incident, or a transmitted, harmonic electromagnetic field. As a general result, the forces are always proportional to the Poynting vector (divided by the velocity of light) times an "equivalent area", which is four times larger than the usual effective area – $3\lambda^2/4\pi$ – of the (tuned) dipole. This clearly implies that the mechanical action depends on the power scattered by the dipole. Similarly, the torque is proportional to the Poynting vector (divided by the angular frequency of the wave) times the same equivalent area.

The existence of the torque, however, is not dependent only on the symmetry properties of the scattering object or on the polarization of the incident wave. We

* On leave of absence from University of Naples, Italy.

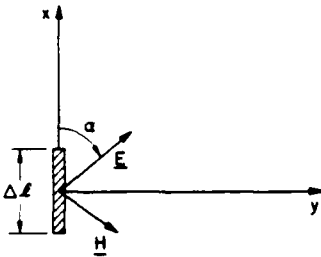


Fig. 1. Receiving electric dipole excited by a monochromatic linearly polarized electromagnetic plane wave

have examined cases in which the incident field – circularly polarized – carries an angular momentum and yet exerts no torque on the dipole. Conversely, we have examined cases in which the dipole – a simple short wire – radiates as a scattered field a linearly polarized wave (in the far-field) and has torques exerted on it. The full analysis of a rigorous boundary value problem – a metal sphere in an incident field – shows that the transient force has not always the same sense as the incident radiation; in other words, the sphere is alternately pushed and pulled in the direction of the incident Poynting vector.

The large variety of effects we discovered in this “case” analysis seems to indicate that this is an underdeveloped field of very interesting research, and a number of general theorems could probably be discovered, thus bringing to a better understanding of a wrongly neglected field.

1. Mechanical Forces and Torques Exerted on a Receiving Dipole by an Incident Electromagnetic Wave

1.1. Linearly Polarized Incident Field

We examine the case of an electric dipole of length $\Delta l \ll \lambda$, tuned on λ , and excited by a normally incident plane monochromatic electromagnetic wave of angular frequency ω and wavelength λ (see Fig. 1). The incident field is linearly polarized; and the electric vector $E \cos \omega t$ makes the angle α with the dipole direction.

Due to the incident field, a current

$$I = \frac{E \cos \alpha \Delta l}{2\pi \zeta \Delta l^2 / 3\lambda^2} \quad (1)$$

is excited along the dipole; and charges

$$Q = \frac{I}{\omega} \sin \omega t \quad (2)$$

of opposite sign appear at its end points. In (1) the expression in the denominator is the radiation resistance of the (tuned) dipole and ζ the free-space intrinsic impedance.

The incident magnetic field, H , interacts with the induced current, thus producing a force

$$\mathbf{F} = \mu I \Delta l \hat{x} \times \mathbf{H} = \frac{E^2}{\zeta c} \frac{3\lambda^2}{2\pi} \cos^2 \alpha \cos^2 \omega t \hat{z} \quad (3)$$

whose time average is given by

$$\langle \mathbf{F} \rangle = \frac{S}{c} A \cos^2 \alpha \hat{z}, \quad A = \frac{3\lambda^2}{2\pi}; \quad S = \frac{1}{2} E H, \quad (4)$$

where c is the light velocity.

Accordingly, the force is given by the radiation pressure S/c times the “effective area” of the unloaded dipole, which is four times larger than the area of a matched dipole

$$A_m = \frac{G\lambda^2}{4\pi} = \frac{3\lambda^2}{8\pi} \quad (5)$$

In addition to the magnetic force, the incident electric field E interacts with the induced charges. No resulting force is produced from this interaction; however, a torque

$$\mathbf{T} = QE \sin \alpha \Delta l \cos \omega t \sin \omega t \hat{z}$$

acts on the dipole. Its time average is given by

$$\langle \mathbf{T} \rangle = 0. \quad (6)$$

Accordingly, no time average torque is exerted on the dipole.

The conclusion is that a linearly polarized electromagnetic wave exerts a force on a receiving dipole tuned on the frequency of the wave, where the force is proportional to the incident power density and is directed along the direction of propagation.

1.2. Circularly Polarized Incident Field

Let us now consider a circularly polarized plane electromagnetic wave which can be conveniently described in the frequency domain by the phasors:

$$\mathbf{E} = E(\hat{x} + i\hat{y}); \quad \mathbf{H} = \frac{E}{\zeta}(\hat{y} - i\hat{x}) \quad (7)$$

incident on the (tuned) dipole. Phasors of currents and charges induced on the dipole are the same as those given by (1) and (2) with $\cos \alpha = 1$ and with the time variation suppressed.

The average force acting on the dipole is still that produced by the interaction of the induced current with the y -component of the magnetic field (the

x-component is ineffective); its time average value is given by

$$\langle F \rangle = \frac{S}{2c} A \hat{z}; \quad S = EH. \quad (8)$$

Note that now the time-average Poynting vector, i.e., the incident power density is doubled compared to the linearly polarized case, and the average force is proportional to one half of the total incident power.

A torque is produced due to the interaction of the y-component of the electric field and the induced charges, hence

$$T = Q i E A l \hat{z}, \quad Q = \frac{I}{i\omega}. \quad (9)$$

This torque has the same sense as the polarization; its time-average value is given by

$$\langle T \rangle = \frac{S}{2\omega} A \quad (10)$$

and therefore is proportional to a torque density – one half of the power density divided by the angular frequency of the wave – times the effective area of the dipole.

The conclusion is that a circularly polarized electromagnetic wave exerts forces and torques on a receiving tuned dipole, in the direction of propagation and in the sense of polarization, respectively; forces as well as torques are proportional to one half of the incident power density.

2. Mechanical Forces and Torques Associated with a Transmitting Dipole

2.1. Linearly Polarized Dipole

We examine the case of an electric dipole of moment p , directed along the x-axis of a reference Cartesian system, as depicted in Fig. 2. The electromagnetic fields associated with the dipole are given, in the frequency domain, by

$$\begin{aligned} E_r &= \frac{p}{\epsilon} \sin \theta \cos \phi \left(\frac{-2i\kappa}{r} + \frac{2}{r^2} \right) \frac{\exp(i\kappa r)}{4\pi r} \\ E_\theta &= \frac{p}{\epsilon} \cos \theta \cos \phi \left(\frac{i\kappa}{r} - \frac{1}{r^2} + \kappa^2 \right) \frac{\exp(i\kappa r)}{4\pi r} \\ E_\phi &= \frac{p}{\epsilon} \sin \phi \left(\frac{i\kappa}{r} - \frac{1}{r^2} + \kappa^2 \right) \frac{\exp(i\kappa r)}{4\pi r} \\ H_\theta &= -i\omega p \sin \phi \left(i\kappa - \frac{1}{r} \right) \frac{\exp(i\kappa r)}{4\pi r} \\ H_\phi &= -i\omega p \cos \theta \cos \phi \left(i\kappa - \frac{1}{r} \right) \frac{\exp(i\kappa r)}{r}, \end{aligned} \quad (11)$$

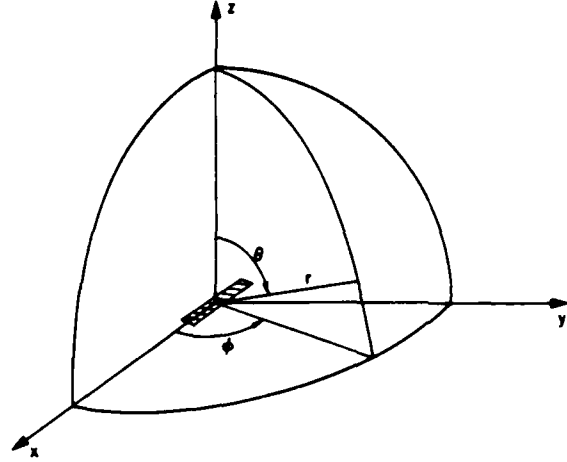


Fig. 2. Linearly polarized transmitting dipole antenna

wherein $\kappa = \omega/c$ and is the free space propagation constant and reference is made to the spherical coordinate system of the figure.

The (time average) force density transmitted by the dipole across the surface $r = \text{const}$ is given by [2]

$$\begin{aligned} \langle f \rangle &= \frac{1}{4} \epsilon (|E_\theta|^2 + |E_\phi|^2 - |E_r|^2) \hat{r} + \frac{1}{4} \mu (|H_\theta|^2 + |H_\phi|^2) \hat{r} \\ &= \frac{1}{4} \frac{\kappa^4}{(4\pi r)^2} \frac{|p|^2}{\epsilon} \left[2(1 - \sin^2 \theta \cos^2 \phi) \right. \\ &\quad \left. - \frac{4}{\kappa^2 r^2} \sin^2 \theta \cos^2 \phi \right. \\ &\quad \left. + \frac{1}{\kappa^4 r^4} (1 - 5 \sin^2 \theta \cos^2 \phi) \right] \hat{r}. \end{aligned} \quad (12)$$

Expression (12) is invariant under the transformation $\theta \rightarrow \pi - \theta$, $\phi \rightarrow \pi - \phi$. Therefore, the (time average) total force transmitted across the half-sphere $r = \text{const}$, $z \geq 0$ is equal and opposite to the total force transmitted across the other half-sphere $r = \text{const}$, $z \leq 0$. The former is given by

$$\begin{aligned} \langle F \rangle &= \hat{z} \int_0^{2\pi} d\phi \int_0^{\pi/2} d\theta r^2 \sin \theta \langle f \rangle \cdot \hat{z} \\ &= \frac{1}{2} \frac{P_T}{c} \left(1 - \frac{1}{\kappa^2 r^2} - \frac{1}{2\kappa^4 r^4} \right) \hat{z}, \end{aligned} \quad (13)$$

wherein P_T is the total power transmitted by the dipole. Note that the component of $\langle F \rangle$ parallel to the plane $z = 0$ is zero. Accordingly, the (time average) total force transmitted across a half-sphere surface is directed along z and changes sign at $\kappa r = 1$. The intensity of this force is proportional to the power radiated by the dipole in the half space $z > 0$, $P_T/2$, divided by the velocity of light.

The (time average) torque density transmitted by the dipole across the surface $r = \text{const}$ is given by [3]

$$\begin{aligned} \langle \mathbf{t} \rangle &= -\frac{1}{2} r \operatorname{Re} \{ \epsilon \mathbf{E}_r \hat{r} \times \mathbf{E}^* + \mu \mathbf{H}_r \hat{r} \times \mathbf{H}^* \} \\ &= -\frac{1}{2} \frac{|p|^2}{\epsilon} \frac{2\kappa^3}{(4\pi r)^2} \\ &\quad \cdot (\hat{\theta} \sin \theta \cos \phi \sin \phi + \hat{\phi} \cos \theta \cos \phi \sin \phi) \\ &\quad \cdot \operatorname{Re} \left\{ 1 + \frac{1}{\kappa^3 r^3} \right\}. \end{aligned} \quad (14)$$

The (time average) total torque $\langle \mathbf{T} \rangle$ transmitted across the half-sphere is equal to zero. Accordingly, a linearly polarized electric dipole transmits no torque and only forces. The dipole is in equilibrium with respect to the transmitted forces.

2.2. Circularly Polarized Dipole

Let us now consider two orthogonal transmitting electric dipoles such that the total dipole moment is given, in the frequency domain, by

$$\mathbf{p} = p(\hat{x} + i\hat{y}). \quad (15)$$

With reference to the spherical system of coordinates of Fig. 2, the field components associated with the dipole are given by

$$\begin{aligned} E_r &= \frac{p}{\epsilon} \sin \theta (\cos \phi + i \sin \phi) \left(-\frac{2i\kappa}{r} + \frac{2}{r^2} \right) \frac{\exp(i\kappa r)}{4\pi r} \\ E_\theta &= \frac{p}{\epsilon} \cos \theta (\cos \phi + i \sin \phi) \left(\frac{i\kappa}{r} - \frac{1}{r^2} + \kappa^2 \right) \frac{\exp(i\kappa r)}{4\pi r} \\ E_\phi &= \frac{p}{\epsilon} (-\sin \phi + i \cos \phi) \left(\frac{i\kappa}{r} - \frac{1}{r^2} + \kappa^2 \right) \frac{\exp(i\kappa r)}{4\pi r} \\ H_\theta &= -i\omega p (\sin \phi - i \cos \phi) \left(i\kappa - \frac{1}{r} \right) \frac{\exp(-i\kappa r)}{4\pi r} \\ H_\phi &= -i\omega p \cos \theta (\cos \phi + i \sin \phi) \left(i\kappa - \frac{1}{r} \right) \frac{\exp(-i\kappa r)}{4\pi r}. \end{aligned} \quad (16)$$

The (time-average) force density transmitted by the dipole across the surface $r = \text{const}$ is now given by

$$\begin{aligned} \langle \mathbf{f} \rangle &= \frac{1}{4} \frac{\kappa^4}{(4\pi r)^2} \frac{|p|^2}{\epsilon} \left[2(1 + \cos^2 \theta) - \frac{4}{\kappa^2 r^2} \sin^2 \theta \right. \\ &\quad \left. + \frac{1}{\kappa^4 r^4} (1 + \cos^2 \theta - 4 \sin^2 \theta) \right] \hat{r}. \end{aligned} \quad (17)$$

Also in this case, and due to the symmetry of (17), the total (time average) force transmitted across the half sphere $r = \text{const}$, $z \geq 0$, is balanced by an equal and opposite force transmitted across the complementary half sphere $r = \text{const}$, $z \leq 0$; and hence the dipole is at rest. The total (time average) force transmitted for $z \geq 0$

is given by

$$\langle \mathbf{F} \rangle = \frac{P_T}{2c} \left(1 - \frac{1}{\kappa^2 r^2} - \frac{1}{2\kappa^4 r^4} \right) \hat{z}. \quad (18)$$

Again, the total (time average) force transmitted is along the z -direction and is proportional to one half of the total transmitted power divided by the velocity of light. Note that for the antenna under consideration the radiation resistance is doubled compared to that of the single dipole.

The (time average) torque density transmitted by the dipole is given by

$$\begin{aligned} \langle \mathbf{t} \rangle &= -\frac{1}{2} \frac{|p|^2}{\epsilon} \frac{\sin \theta 2\kappa^3}{(4\pi r)^2} \operatorname{Re} \left\{ \left(1 - i \frac{1}{\kappa^3 r^3} \right) \hat{\theta} \right. \\ &\quad \left. - \left(i + \frac{1}{\kappa^3 r^3} \right) \cos \theta \hat{\phi} \right\}. \end{aligned} \quad (19)$$

The total torque transmitted across the half-sphere $r = \text{const}$, $z \geq 0$ is readily computed as

$$\langle \mathbf{T} \rangle = \frac{P_T}{2\omega} \hat{z}. \quad (20)$$

The torque transmitted across the complementary half-sphere is the same. Accordingly, the dipole is not in equilibrium as far as torques are concerned.

3. Mechanical Forces and Torques Associated with a Moving Dipole

3.1. Translating Dipole

We examine the case of an electric (tuned) dipole, excited by an electromagnetic plane wave, as depicted in Fig. 1. We are taking the angle α to be zero for convenience, and we assume the dipole to move with a constant velocity $\mathbf{v} = -v\hat{z}$ along the negative z axis. It is evident that the force acting on the dipole is given by the same expression (4) with $\alpha = 0$, provided that the Poynting vector \mathbf{S} is computed in a reference frame fixed to the dipole.

If \mathbf{E}' , \mathbf{H}' are the electromagnetic fields in this frame, we have

$$\begin{aligned} \mathbf{E}' &= (\mathbf{E} + \mathbf{v} \times \mu \mathbf{H}) \frac{1}{\sqrt{1 - \beta^2}} \\ \mathbf{H}' &= (\mathbf{H} - \mathbf{v} \times \epsilon \mathbf{E}) \frac{1}{\sqrt{1 - \beta^2}}, \end{aligned} \quad (21)$$

wherein $\beta = v/c$. Then, after a few computations, we get the following expression for the Poynting vector in the primed frame (fixed to the dipole)

$$\mathbf{S}' = \mathbf{S} \frac{1 + \beta}{1 - \beta}. \quad (22)$$

This, however, does *not* imply that the average force exerted upon the dipole is increased by the scalar factor appearing in (22) in comparison to the case of the dipole at rest. As a matter of fact, the incident wave in the primed reference frame has a Doppler shifted frequency

$$f' = f \sqrt{\frac{1+\beta}{1-\beta}} \quad (23)$$

Accordingly, the effective area of the dipole - see (4) - takes the new value

$$A' = A \frac{1-\beta}{1+\beta} \quad (24)$$

When the dipole is retuned on the new frequency, the force acting upon it remains constant.

3.2. Rotating Dipole

We examine now the case of an electric (tuned) dipole, excited by an electromagnetic plane wave, as depicted in Fig. 3. The dipole is rotating with constant angular velocity Ω along the z -axis, so that the dipole makes with respect to the x -axis an angle ϕ given by

$$\phi = \Omega t \quad (25)$$

We can compute the forces and torques acting on the rotating dipole in the following manner. We transform the pertinent results of Sect. 1 from the inertial laboratory frame of Sect. 1 to the non-inertial rest frame of the rotating dipole and then neglect manifestly small correction terms. Usually the procedure of transforming from inertial frames to non-inertial frames or vice versa is a long calculation, but in the case of present interest simplifying approximations can be introduced and the procedure can accordingly be shortened. In particular, we are interested in the components

$$E_\phi = E \cos \phi; \quad E_\psi = -E \sin \phi; \quad H_\phi = \frac{E}{\zeta} \cos \phi \quad (26)$$

which, upon transformation to the rotating reference frame, are given by [4]

$$E'_\phi = E_\phi; \quad E'_\psi = \frac{E_\psi}{\sqrt{1-\beta^2}}; \quad H'_\phi = \frac{H_\phi}{\sqrt{1-\beta^2}}, \quad (27)$$

wherein the parameter

$$\beta = \Omega Q/c \quad (28)$$

takes into account the relativistic correction. However, when the fields are evaluated at the rotating elementary dipole, we have $\Delta l \rightarrow 0$, $q \rightarrow 0$ and $\beta \rightarrow 0$. Accordingly, the force acting on the dipole is given by

$$\mathbf{F} = \frac{E^2}{\zeta c} A \cos^2 \phi \hat{z} \quad (29)$$

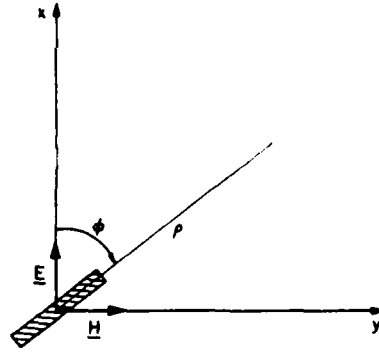


Fig. 3. Receiving rotating electric dipole excited by a linearly polarized electromagnetic field

In order to consider the time average of (29), it should be remarked that the fields are changing in time with an angular frequency ω and so the quantity to be averaged is $\cos^2 \omega t \cos^2 \Omega t$. If the average is made with respect to the period $2\pi/\omega$ of the incident wave, then, after some lengthy algebra, we get

$$\langle \mathbf{F} \rangle = \frac{S}{2c} A \hat{z} \left\{ 1 + \frac{\sin \frac{2\pi\Omega}{\omega}}{\frac{2\pi\Omega}{\omega}} \left[\cos \left(2\Omega t + \frac{2\pi\Omega}{\omega} \right) - \frac{\Omega/\omega}{1 - (\Omega/\omega)^2} \sin(2\omega t) \sin \left(2\Omega t + \frac{2\pi\Omega}{\omega} \right) - \frac{(\Omega/\omega)^2}{1 - (\Omega/\omega)^2} \cos(2\omega t) \cos \left(2\Omega t + \frac{2\pi\Omega}{\omega} \right) \right] \right\} \quad (30)$$

If $\Omega/\omega \ll 1$, the term in the curly brackets is approximately equal to

$$1 + \cos(2\Omega t); \quad (31)$$

and, after another time average with respect to the period $2\pi/\Omega$, we recover the result (8). When $\Omega/\omega = 1$, the term in the curly brackets equals 3/2.

To evaluate the torque acting on the dipole, we first compute the charges (of opposite sign) at the endpoints of the dipole, hence

$$Q = \frac{E \Delta l}{2\pi \zeta \Delta l^2 / 3\lambda^2} \int \cos \omega t \cos \Omega t dt = \frac{E \Delta l}{2\pi \zeta \Delta l^2 / 3\lambda^2} \frac{\omega \sin \omega t \cos \Omega t - \Omega \cos \omega t \sin \Omega t}{\omega^2 - \Omega^2} \quad (32)$$

Then, the (instantaneous) torque is given by

$$\mathbf{T} = Q E_\psi \Delta l \hat{z} = \frac{E^2}{\zeta} A \hat{z} \cos \omega t \sin \Omega t \frac{\omega \sin \omega t \cos \Omega t - \Omega \cos \omega t \sin \Omega t}{\omega^2 - \Omega^2}$$

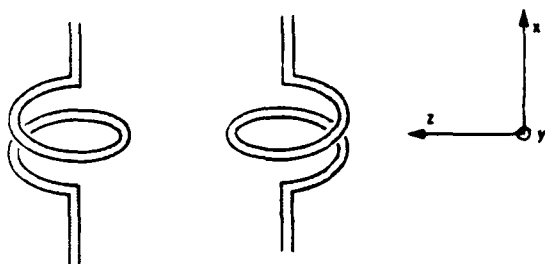


Fig. 4. (a) and (b) Two chiral dipoles

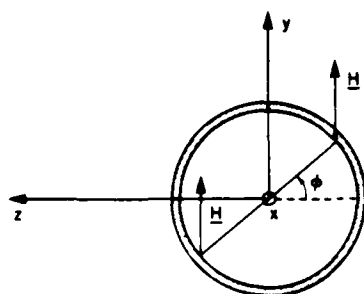


Fig. 5. Geometry of interaction between the magnetic field and the loop of the chiral dipole

By similarly averaging over the period $2\pi/\omega$, we get

$$\begin{aligned} \langle T \rangle = \frac{S}{2\omega} A \frac{\omega/\Omega}{1 - (\Omega/\omega)^2} & \left\{ 1 - \frac{\sin \frac{2\pi\Omega}{\omega}}{\frac{2\pi\Omega}{\omega}} \left[\cos \left(2\Omega t + \frac{2\pi\Omega}{\omega} \right) \right. \right. \\ & - \frac{1 + (\Omega/\omega)^2}{1 - (\Omega/\omega)^2} \cos 2\omega t \cos \left(2\Omega t + \frac{2\pi\Omega}{\omega} \right) \\ & \left. \left. - \frac{2\Omega/\omega}{1 - (\Omega/\omega)^2} \sin 2\omega t \sin \left(2\Omega t + \frac{2\pi\Omega}{\omega} \right) \right] \right\}. \quad (34) \end{aligned}$$

When $\Omega/\omega \ll 1$, the term in the curly brackets is approximately equal to

$$1 - \cos(2\Omega t) \quad (35)$$

and, after another time average, we recover the result (10) weighted by the factor $\Omega/\omega \ll 1$. When $\Omega/\omega = 1$, the term in the curly brackets is proportional to $[1 - (\Omega/\omega)^2]^2$; therefore, the average torque is zero.

4. Mechanical Forces and Torques Exerted on a Receiving Chiral Dipole by an Incident Electromagnetic Wave

4.1. Linearly Polarized Incident Field

Let us consider two *chiral dipoles* [5] as depicted in Fig. 4. We will define as *right-handed* the chiral dipole "b", while the chiral dipole "a" is defined as *left-handed*. In addition, the dipoles will be defined as *balanced* if the following relation exists between the length Δl of the (electric) dipole and the area πa^2 of the (magnetic) dipole

$$\Delta l = \kappa N \pi a^2 = \frac{2\pi^2 N a^2}{\lambda}, \quad (36)$$

wherein N is the number of turns of the loop. Under these circumstances, the far field radiated by the chiral dipoles is everywhere circularly polarized, and the radiation resistance is twice as large as that of the single electric dipole.

We examine now the case of a linearly polarized electromagnetic field described, in frequency domain, by

$$\mathbf{E} = E \hat{x}, \quad \mathbf{H} = \frac{E}{\zeta} \hat{y} \quad (37)$$

and incident upon the (tuned) dipoles. Each dipole will be subject to a z -directed force which can be computed as in Sect. 1, with the only difference being the new radiation resistance. Hence

$$\langle F \rangle = \frac{S}{2c} A \hat{z}, \quad (38)$$

wherein A is given by (4), as usual. Equation (38) coincides with (8).

Now, at variance with the single dipole, the current circulating in the loop,

$$\frac{E \Delta l}{4\pi \zeta \Delta l^2 / 3\lambda^2} \quad (39)$$

will interact with the incident magnetic field, thus producing an (instantaneous) torque (see Fig. 5)

$$\begin{aligned} T &= \frac{E^2}{\zeta} A \frac{N a^2 \sqrt{\mu \epsilon}}{\Delta l} \int_0^\pi \pm \hat{\phi} \sin \phi d\phi \\ &= \pm \frac{E^2}{2\zeta \omega} A. \quad (40) \end{aligned}$$

Here use has been made of (36) and the upper and lower signs refer to the right-handed and left-handed dipoles respectively. Accordingly, the (time average) torque is given by

$$\langle T \rangle = \pm \frac{S}{2\omega} A \quad (41)$$

which is identical to (10).

4.2. Circularly Polarized Incident Field

We examine now the case of an incident wave circularly polarized along the z -direction, i.e., in complex notation,

$$\mathbf{E} = E(\hat{x} + i\hat{y}); \quad \mathbf{H} = \frac{E}{\zeta}(\hat{y} - i\hat{x}). \quad (42)$$

This wave is incident upon a balanced (tuned) chiral dipole, either right-handed or left-handed. The open circuit voltage induced by the electric field (along the electric dipole) is given by $E\Delta l$. Similarly, the open circuit voltage induced by the magnetic field in the loop is given by

$$iN \frac{E}{\zeta} (-i\omega) = E\Delta l, \quad (43)$$

upon use of the balance condition (36). Then, examination of Fig. 4 clearly shows that the two voltages add for the right-handed chiral dipole, while they cancel out for the left-handed one. Accordingly, one of the two dipoles is "invisible" to the incident circularly polarized wave, and no force or torque is acting upon it. On the contrary, the current

$$I = \frac{E\Delta l}{2\pi\zeta\Delta l^2/3\lambda^2} \quad (44)$$

is induced on the other dipole. This current will interact with the incident magnetic field thus producing an average force

$$\langle \mathbf{F} \rangle = \frac{S}{2c} A \hat{z} \quad (45)$$

equal to (8). Note that the forces due to the interaction of the magnetic field with the current along the loop have a zero spatial average.

Now, we compute the torque acting on the dipole. This is produced in part by the y -component of the magnetic field interacting with the current along the loop. Hence

$$T_1 = \hat{z} \frac{E^2}{\zeta\omega} A \quad (46)$$

and, in part, by the y -component of the electric field interacting with the charges at the end-points of the wire. Hence

$$T_2 = \hat{z} \frac{E^2}{\zeta\omega} A. \quad (47)$$

Accordingly, the average total torque is given by

$$\langle \mathbf{T} \rangle = \hat{z} \frac{S}{\zeta} A \quad (48)$$

which is twice as large as (10).

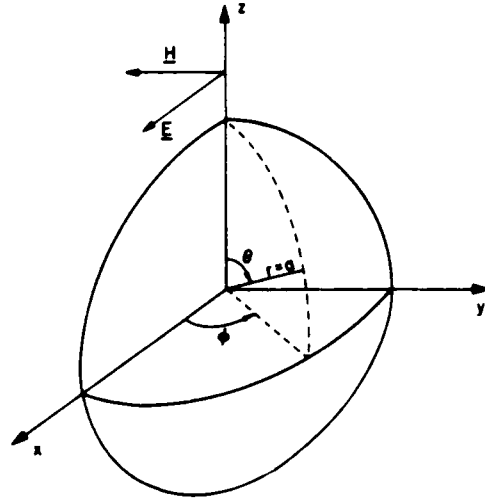


Fig. 6. Excitation of a metal sphere by a plane wave

5. A Rigorous Boundary Value Solution. Mechanical Action on a Metal Sphere Produced by an Electromagnetic Pulse

We examine the case of a metal sphere excited by a plane electromagnetic wave as depicted in Fig. 6. For a steady-state incident field, the total field components on the spherical surface $r=a$ are given by [6]

$$E_r = -\frac{E \cos \phi}{(\kappa a)^2} \sum_{n=1}^{\infty} (-i)^n (2n+1) \frac{P_n^1(\cos \theta)}{[\kappa a h_n^{(1)}(\kappa a)]}, \quad (49)$$

$$H_\theta = \frac{1}{\zeta} T_1(\theta) \sin \phi; \quad H_\phi = \frac{1}{\zeta} T_2(\theta) \cos \phi,$$

wherein

$$T_1(\theta) = \frac{E}{\kappa a} \sum_{n=1}^{\infty} (-i)^{n+1} \frac{2n+1}{n(n+1)} \left\{ \frac{1}{[\kappa a h_n^{(1)}(\kappa a)]'} \frac{P_n^1(\cos \theta)}{\sin \theta} - \frac{i}{[\kappa a h_n^{(1)}(\kappa a)]'} \frac{dP_n^1(\cos \theta)}{d\theta} \right\} \quad (50)$$

$$T_2(\theta) = \frac{E}{\kappa a} \sum_{n=1}^{\infty} (-i)^{n+1} \frac{2n+1}{n(n+1)} \left[\frac{1}{[\kappa a h_n^{(1)}(\kappa a)]'} \frac{dP_n^1(\cos \theta)}{d\theta} - \frac{i}{[\kappa a h_n^{(1)}(\kappa a)]'} \frac{P_n^1(\cos \theta)}{\sin \theta} \right]$$

and a prime implies the derivative operation with respect to the argument¹.

Let $E(\omega)$ be the spectral distribution of the incident field, i.e.,

$$E = E_0 \mathcal{E}(\omega) \exp(ikz), \quad (51)$$

wherein E_0 is a convenient normalization constant, and $\tau = a/c$. Let us further introduce the following

¹ Note a misprint error in the expression for E_r in [6].

time-dependent functions

$$\begin{aligned} f_n(t) &= \int_{-\infty}^{\infty} \frac{\mathcal{E}(\omega) \exp(-i\omega t) (-i)^{n+1}}{(\omega\tau) [\omega\tau h_n^{(1)}(\omega\tau)]} d\omega \\ g_n(t) &= \int_{-\infty}^{\infty} \frac{\mathcal{E}(\omega) \exp(-i\omega t) (-i)^{n+2}}{(\omega\tau) [\omega\tau h_n^{(1)}(\omega\tau)]} d\omega \\ \tilde{f}_n(t) &= \frac{1}{\tau} \int_{-\infty}^{\infty} f_n(t) dt \end{aligned} \quad (52)$$

Then, the transient field at the sphere surface $r=a$ is given by

$$\begin{aligned} E_r &= -E_0 \cos \phi \sum_{n=1}^{\infty} (2n+1) \tilde{f}_n(t) P_n^1(\cos \theta) \\ H_\theta &= \frac{E_0 \sin \phi}{\zeta} \sum_{n=1}^{\infty} \frac{2n+1}{n(n+1)} \left[f_n(t) \frac{P_n^1(\cos \theta)}{\sin \theta} \right. \\ &\quad \left. + g_n(t) \frac{dP_n^1(\cos \theta)}{d\theta} \right] \\ H_\phi &= \frac{E_0 \cos \phi}{\zeta} \sum_{n=1}^{\infty} \frac{2n+1}{n(n+1)} \left[f_n(t) \frac{dP_n^1(\cos \theta)}{d\theta} \right. \\ &\quad \left. + g_n(t) \frac{P_n^1(\cos \theta)}{\sin \theta} \right] \end{aligned} \quad (53)$$

Transient surface density charges

$$\rho_s = \epsilon E_r \quad (54)$$

and surface density currents

$$J_s = -H_\phi; \quad J_\phi = H_\theta \quad (55)$$

are excited on the sphere surface. The electric field will interact with the charges, thus producing a force density

$$f_r = \epsilon E_r^2 \hat{r} \quad (56)$$

and the magnetic field will interact with the currents, thus producing a force density

$$f_m = -\mu(H_\theta^2 + H_\phi^2) \hat{r} \quad (57)$$

For the first force density we have

$$\begin{aligned} f_r &= \epsilon E_0^2 \cos^2 \phi \sum_{n=1}^{\infty} \sum_{m=1}^{\infty} (2n+1)(2m+1) \tilde{f}_n(t) \tilde{f}_m(t) \\ &\quad \frac{P_n^1(\cos \theta)}{\sin \theta} \frac{P_m^1(\cos \theta)}{\sin \theta} \end{aligned} \quad (58)$$

This force density has a $\cos^3 \phi$ dependence for its x -component; and a $\cos^2 \phi \sin \phi$ dependence for its y -component. Therefore, the space-average of these two components is zero. This does not happen for the z -component of (58), whose ϕ -dependence is of type $\cos^2 \phi$. Accordingly, the (space average) total force

acting on the sphere has only a z -component given by

$$\begin{aligned} F_z &= \hat{z} \frac{S}{c} \pi a^2 \sum_{n=1}^{\infty} \sum_{m=1}^{\infty} (2n+1)(2m+1) f_n(t) \tilde{f}_m(t) \\ &\quad \cdot \int_0^\pi \cos \theta \sin \theta P_n^1(\cos \theta) P_m^1(\cos \theta) d\theta, \end{aligned} \quad (59)$$

wherein $S = E_0^2/\zeta$.

By repeated use of recurrence and orthogonality relations [7], it can be shown that the integral appearing in (59) is different from zero only for $m=n+1$ and $m=n-1$. Then, rearranging the terms of the series, we get

$$F_z = \hat{z} \frac{S}{c} 4\pi a^2 \sum_{n=1}^{\infty} n(n+1)(n+2) \tilde{f}_n(t) \tilde{f}_{n+1}(t). \quad (60)$$

For the second density force we proceed similarly. The x and y components of the (space-average) total force acting upon the sphere are zero, and only the z -component is different from zero. This last component is given by

$$\begin{aligned} F_m &= -\hat{z} \frac{S}{c} \pi a^2 \sum_{n=1}^{\infty} \sum_{m=1}^{\infty} \frac{2n+1}{n(n+1)} \frac{2m+1}{m(m+1)} \left[(f_n f_m + g_n g_m) \right. \\ &\quad \cdot \int_0^\pi \left(\frac{P_n^1}{\sin \theta} \frac{P_m^1}{\sin \theta} + \frac{dP_n^1}{d\theta} \frac{dP_m^1}{d\theta} \right) \cos \theta \sin \theta d\theta \\ &\quad \left. + (f_n g_m + f_m g_n) \int_0^\pi \left(\frac{P_n^1}{\sin \theta} \frac{dP_m^1}{d\theta} + \frac{P_m^1}{\sin \theta} \frac{dP_n^1}{d\theta} \right) \right. \\ &\quad \left. \cdot \cos \theta \sin \theta d\theta \right]. \end{aligned} \quad (61)$$

The integral which appears in (61) can be evaluated upon repeated use of recurrence relationship between associated Legendre polynomials and of their defining differential equation [8]. In particular, the second integral is different from zero only for $n=m$; and the first one only for $m=n+1$ and $m=n-1$. Then, upon rearranging the terms of the series, we get

$$\begin{aligned} F_m &= -\hat{z} \frac{S}{c} 4\pi a^2 \sum_{n=1}^{\infty} \left[\frac{n(n+2)}{n+1} (f_n f_{n+1} + g_n g_{n+1}) \right. \\ &\quad \left. + \frac{2n+1}{n(n+1)} f_n g_n \right]. \end{aligned} \quad (62)$$

Accordingly, the (space-average) total force acting on the sphere is given by

$$\begin{aligned} F &= -\hat{z} \frac{S}{c} 4\pi a^2 \sum_{n=1}^{\infty} \left[\frac{n(n+2)}{n+1} (f_n f_{n+1} + g_n g_{n+1}) \right. \\ &\quad \left. + \frac{2n+1}{n(n+1)} f_n g_n - n(n+1)(n+2) \tilde{f}_n \tilde{f}_{n+1} \right]. \end{aligned} \quad (63)$$

An interesting case is that of a bandlimited signal such that $\omega_m a < 1$, ω_m being the maximum angular frequency. Then, using the series expansion

$$x h_n^{(1)}(x) \simeq \frac{\exp(ix)}{i^{n+1}} \frac{(2n)!}{n!} \frac{1}{(2ix)^n} \quad (64)$$

it follows that, to the lowest order in $\tau\partial/\partial t$

$$\begin{aligned} E_0 f_n(t) &\simeq (-)^{n-1} (2\tau)^n \frac{n!}{n(2n)!} \frac{\partial^n E}{\partial t^n} \Big|_{t=t^*, z=0} \\ E_0 g_n(t) &\simeq (-)^{n-1} (2\tau)^{n-1} \frac{n! 2}{(2n)!} \frac{\partial^{n-1} E}{\partial t^{n-1}} \Big|_{t=t^*, z=0} \\ E_0 \vec{f}_n(t) &\simeq \frac{1}{n} g_n(t), \quad t^* = t + \frac{a}{c}, \end{aligned} \quad (65)$$

where, now, $E = E(t)$ and is the time-varying incident field. Accordingly, at the lowest order again

$$\begin{aligned} \vec{F} &= -\hat{z} \frac{1}{\zeta c} 4\pi a^2 2\tau E(t^*) \frac{\partial E}{\partial t} \Big|_{t=t^*, z=0} \\ &= -\frac{4\pi a^2}{c} \tau \frac{\partial S}{\partial t} \Big|_{t=t^*} \end{aligned} \quad (66)$$

where $S(t)$ is the instantaneous value of the incident Poynting vector at $z=0$. Note that, at the lowest considered order, the time average of \vec{F} is equal to zero for a sinusoidal incident field, since the sphere does not scatter any real power. For a Gaussian pulse

$$E(z, t) = E_0 \exp \left[-\frac{(t + z/c)^2}{2T^2} \right], \quad (67)$$

$$\vec{F}(t) = \hat{z} \frac{S(t^*)}{c} 4\pi a^2 \frac{2\tau t^*}{T^2}. \quad (68)$$

It is seen that the sphere is first pushed ($t^* < 0$) in the sense of propagation of the incident wave; and then pulled ($t^* > 0$).

6. Conclusions

We have considered the mechanical effects that an electromagnetic wave can have on various types of targets. Using nothing more than the Lorentz force, given by $\vec{F} = q\vec{E} + \vec{J} \times \mu\vec{H}$, we have found that

- a linearly polarized wave falling on a tuned electric-receiving dipole will exert a body force – see (4) – on the dipole in the direction of incidence,
- a circularly polarized wave falling on such a dipole will exert not only a body force but also a torque – see (10).

We also found that

- for a fixed transmitting dipole surrounded by an absorbing spherical surface of radius r , there is no recoil force on the dipole but there is a force on the absorbing spherical surface – see (13) – which tends to make it implode when $\kappa r < 1$ and explode when $\kappa r > 1$. Moreover,

- when the fixed transmitting antenna happens to be a turnstile, there is a recoil torque on the antenna, and a torque on the absorbing spherical surface – see (26),

and again there are the implosive and explosive forces as before.

In addition, we have studied the problem of a receiving dipole that is either moving at constant velocity or simply rotating. We have found that

- when the tuned dipole is in pure translational motion, the force exerted on the dipole by the incident signal is equal to that on the tuned dipole at rest.

- When the dipole is only rotating, the incident signal exerts also a torque on the spinning dipole – see (34).

For a balanced chiral dipole receiving antenna in the field of a linearly polarized incident wave, we deduced that

- the body force exerted on the antenna is independent of the handedness of the antenna – see (38), whereas the torque changes sign with a change of handedness. If such an antenna is exposed to a circularly polarized incident wave, then

- the antenna is completely free of body force and torque for one handedness, but not for the other – see (45) and (48). That is, with the proper handedness the antenna is “invisible” at the “balanced” frequency.

Finally, the push-pull effect has been examined for the case of a pulse falling on a spherical target. It has been found that

- the leading term of body force excited on the sphere by the incident pulse is proportional to $\partial S/\partial t$, provided that the effective bandwidth of the pulse multiplied by the characteristic time of the target is less than unity.

Acknowledgments. The authors appreciate the kind assistance of Dr. J.P. Castillo, Kirtland Air Force Base, New Mexico and of K.S.H. Lee, Dikewood Corporation, Santa Monica, California. This work was supported by the U.S. Air Force Office of Scientific Research under Grant No. AFOSR-77-3451.

References

- R.A. Valitov (ed.): *Ponderomotornoye Deystviye Elektromagnitnogo Polya* (Ponderomotive Effects of Electromagnetic Fields) (Sovetskoye Radio Press, Moscow 1975)
- J.A. Stratton: *Electromagnetic Theory* (McGraw-Hill, New York 1941) pp. 103–104
- N. Carrara, T. Fazzini, L. Ronchi, G. Toraldo di Francia: “Sul momento di rotazione del campo elettromagnetico”, *Alta Frequenza* **24**, 100–109 (1955)
- J. Van Bladel: *Proc. IEEE* **64**, 301–318 (1976)
- D.J. Jaggard, A.A. Mickelson, C.H. Papas: *Appl. Phys.* **18**, 211–216 (1979)
- J.J. Bowman, T.B.A. Senior, P.L.E. Uslenghi: *Electromagnetic and Acoustic Scattering by Simple Shapes* (North-Holland Publishing, Amsterdam 1969) pp. 396–397
- M. Abramovitz, I.A. Stegun: *Handbook of Mathematical Functions* (NBS Applied Mathematical Series, 1954) p. 334, Eqs. (8.14.11) and (8.14.13)
- Abramovitz et al.: *Loc. cit.*, p. 334, Eq. (8.5.4)

DATE
LME